ADDIS ABABA UNIVERSITY-ADDIS ABABA INSTITUTE OF TECHNOLOGY

SCHOOL OF CIVIL AND ENVIRONMENTAL ENGINEERING

Tension Property of Concrete and its Role in the Immediate Deflection of Reinforced Concrete Beams under Serviceability Limit State

A Thesis in Structural Engineering

By Yisshak Tadesse

14/12/2015

Addis Ababa

Submitted in Partial Fulfillment of the Requirements for the **Degree of Master of Science**

ADDIS ABABA UNIVERSITY-ADDIS ABABA INSTITUTE OF THECHNOLOGY
SCHOOL OF CIVIL AND ENVIRONMENTAL ENGINEERING

"Tension Property of Concrete and its Role in the Immediate Deflection of Reinforced Concrete Beam under Serviceability Limit State"

By

Yisshak Tadesse

Approved by the Board of Examiners:

Esayas Gebreyouhannes (PhD)	_____	_____
Advisor	**Signature**	**Date**
Asnake Adamu (PhD)	_____	_____
Internal Examiner	**Signature**	**Date**
Girma Zerayohannes (PhD)	_____	_____
External Examiner	**Signature**	**Date**
Nebiyu Siraj	_____	_____
Chairman	**Signature**	**Date**

Acknowledgement

I would like to forward my deepest appreciation and gratitude to my advisor Esayas Gebreyouhannes (PhD) for his patience and constructive advice throughout the course of the thesis. Not only did he help me with invaluable advice, I have also learned a lot from him.

I would also like to thank the following people for their support, Ato Dawit Kebede, CEO of Afro European Engineers for his understanding, W/rt Mekdes Tadesse and all the AAiT staff.

Last but certainly not least, I would like to thank my family members and friends for their invaluable support.

TABLE OF CONTENTS

LIST OF TABLES

LIST OF FIGURES

LIST OF EQUATIONS

ABSTRACT

Modeling the behavior of cracked tensile concrete is a complicated issue. Due to bond with reinforcement, the concrete between cracks carries a certain amount of tensile force normal to the cracked plane. The concrete adheres to reinforcement bars and contributes to overall stiffness of the structure. The phenomenon, called tension-stiffening, has significant influence on the results of short-term deformational analysis. The main objective of this thesis is to investigate the current norms of calculating deflection and propose a free-of-shrinkage deflection calculation alternative that incorporates tension-stiffening law for flexural reinforced concrete (RC) members subjected to short-term loading.

It consists of an introduction, four Chapters and general conclusions. Reasons for investigation and main objective are discussed in the first Chapter. The second Chapter presents literature review on deformational models of RC members. Furthermore design code and numerical methods for determining deflections of reinforced concrete members are reviewed.

The third Chapter presents the current practice of calculating deflection along the span of a beam. This is accomplished by taking a representative simply supported beam with expected set of loads acting on it. The influence of shrinkage is not included to emphasize on the role of the concrete in tension of RC members subjected to short-term loading. A numerical procedure has been carried out for computing free-of-shrinkage deflection of the beam using the current two most prevalent codes; ACI 318 and EC2, as well as prominent deflection calculation approach (Bischoff's Method).

The fourth Chapter presents the findings of an experimental investigation as a stepping stone to point out the role of concrete in the tension zone of a reinforced concrete section under flexure. Also two approaches are discussed to include the tension stiffening effect. First, the effective stiffness approach where the modulus of elasticity of steel is modified to incorporate the tension stiffening role, and later the modeling of the post–crack tensile property of concrete and quantify its effect in relation to the area of concrete in the tension zone. This is followed by a proposed method of using the two approaches to come up with a procedure to compute the deflection of RC beam which is more practical and refined. The result of the approach is compared with that of the results computed in Chapter three. The fifth

Chapter presents the comparison and discussion of the predictions made in Chapter three and four and the proposed model. Recommendations are expressed at the end of the Chapter.

1. Introduction

1.1 Motivation

The use reinforced concrete as a primary construction material in Ethiopia has been the trend for the past four decades. And in the design of a reinforced structure, the governing standards typically require that the structural elements be proportioned according to the results of linear elastic analysis. The achieved design usually meets strength and serviceability criteria, though perhaps not most efficiently. During the life of the structure, however, situations may arise where a more accurate assessment of the structure's strength and expected behavior like deflection is required. This is particularly true in instances where the structure is required to be economical and yet function safely. The current norm in Ethiopia on establishing the deflection of structural members is very limited and unaddressed as designers choose to avoid going through the trouble of computing the deflection by limiting the span to depth ratio.

Deflection is a response of a structure which most of its attributes belong to the non-linear behavior of the concrete and that of the steel. Such behavior is referred as non-linear since the relationship between the stress and strain will be past the linear relationship stage. To address such concerns, advanced nonlinear methods of analysis must be employed. Thus, there is a growing need for analysis tools and simplified approaches that nearly simulate the reality if not accurately model the performance of reinforced concrete structures.

1.2 Objective

The objective of this thesis is to develop analysis and design recommendations in determining the short term deflection of reinforced concrete beams with due consideration to the role of the concrete in the tension zone.

1.3 Scope of the research

This thesis focuses on the immediate/short-term deflection of a reinforced concrete flexural element (i.e. beams and/or one way slab system). This is to emphasize on the role of concrete in tension for such elements and reduce the long term effects resulting from shrinkage and creep. Such approach was used as it will show the objective of the thesis clearly.

2. Literature Review on Deflection of Reinforced Concrete Flexural Members

2.1 Mechanics of Reinforced Concrete

The behavior exhibited by a cracked reinforced concrete beam under flexure is a complex process that entails a wide range of effects, such as, different strength and deformation properties of steel and concrete, cracks that will inevitably occur, tension-softening and tension-stiffening, bond slip between reinforcement and concrete, etc. The constitutive models for concrete have been developed all over the world, and this paper tries to makes use of selected laws with the aim to meet the objective of the research.

2.1.1 Uniaxial Compression

Concrete is a composite material composed of aggregate, generally sand and gravel, chemically bound together by hydrated portland cement (James K. wight and James G. macgregor 6th Edition, [1]). The response of concrete in uniaxial compression is usually obtained from cylinders with a height to diameter ratio of 2 to 1 or from cubes. A standard cylinder is 300 mm high by 150 mm diameter and the lower characteristics value of its compressive strength at 28 days is termed f_{ck}. This is the value of compressive strength exceeded by 95 % of all standard cylinder specimens tested at 28 days under standard conditions (Gilbert 2002). Smaller cylinders, or cubes, (generally having a higher compressive strength) are also used for production control, the results of which can be converted into equivalent standard cylinder strength values using appropriate conversion factors.

Although concrete is made up of essentially elastic, brittle materials, its stress–strain curve is nonlinear and appears to be somewhat ductile. This can be explained by the gradual development of micro-cracking within the concrete and the resulting redistribution of stress from element to element in the concrete.

Response under compression in the post-peak range follows a softening or descending branch until the concrete reaches its ultimate strain. Strain softening under compression is influenced by specimen size, strength of the concrete, and the stiffness of the testing machine.

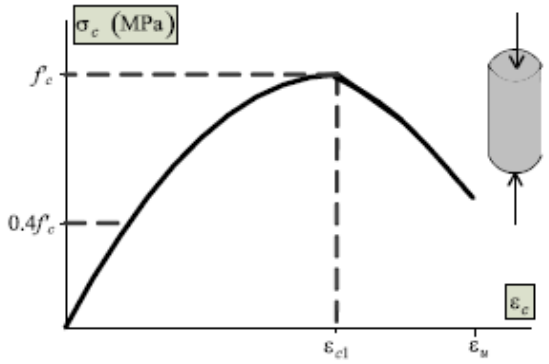

Figure 2-1Typical uniaxial stress-strain curves of concrete in compression

2.1.2 Uniaxial Tension

The tensile strength of concrete is only a fraction of it compressive strength and is defined as the maximum stress that concrete can withstand when subjected to uniaxial tension. It becomes hard to measure direct uniaxial tensile strength because it is difficult to achieve true axial tension without secondary stresses caused by the holding devices. The commonly used methods, to determine tensile strength, are the cylinder splitting or Brazilian test, and the flexural or modulus of rupture test.

Hughes & Chapman (1966) and Evans & Marathe (1968) have used modified direct tension testing machines to obtain stress-strain diagrams in tension with ascending and descending branches similar to those obtained in compression. The shape of the curve (Figure 2-2) shows many similarities to the uniaxial-compression curve (Figure 2-1); however, there are some differences. The curve shown in Figure 2-2 is nearly linear up to a relatively higher stress level. The stress of about 60 % of the uniaxial tensile strength, f_{ct}, can be considered as a limit of elasticity. The interval of stable crack propagation is relatively short and the limit of unstable crack propagation is reached at about 75 % of f_{ct} (Evans & Marathe 1968). The failure in tension is caused by a few bridging cracks rather than by numerous cracks, as it is for the compressive states of stress.

The ratio between uniaxial tensile and compressive strength may vary considerably but usually ranges between 0.05 and 0.1. The modulus of elasticity under uniaxial tension is somewhat higher and the Poisson's ratio somewhat lower than in uniaxial compression. In fracture mechanics approach, based on crack growth and localized effects, the shape of the strain softening curve in tension is adjusted from one problem to another, depending on fracture energy (e.g. Bazant & Oh 1983, Wittmann 2002, Liu et al 2008, Darwin et al 2001). Massicote et al. (1988)

performed a detailed analysis of 52 test results presented by Gopalaratnam & Shah (1985), Hilleborg (1983, 1985a, b), Guo & Zhang (1986), Bazant & Oh (1983) and Yankelevsky & Reinhardt (1987). Based on these results and as a reasonable compromise between accuracy and simplicity, a trilinear stress-strain curve was adopted (Massicotte 1988), with a linear ascending branch and a bilinear softening branch after cracking. The change of slope in the descending branch occurs at one-third of f_{ct}, as proposed by Hilleborg (1985).

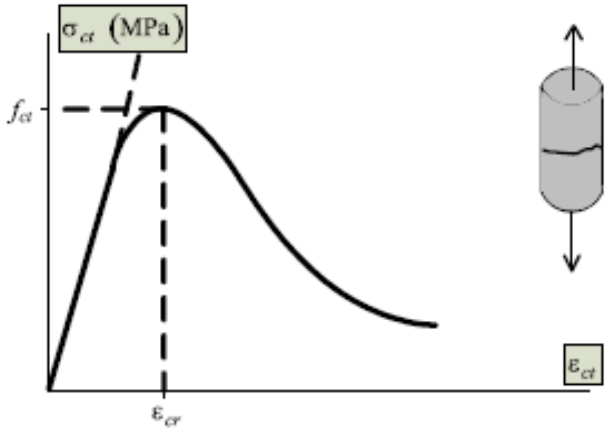

Figure 2-2 Uniaxial tensile stress-strain curves of concrete

In this thesis the smeared stress strain relationship of concrete in tension is used. This will be further discussed in section 4.3.1.

2.1.3 Steel Reinforcement

Steel reinforcement is used to provide strength, ductility and serviceability to concrete structures. With regard to serviceability, reinforcement is used to reduce instantaneous and long-term deformations and provide crack control.

Structural concrete elements are generally designed such that failure will be governed by yielding of the reinforcement. The yield stresses typically amount to 400 - 600 MPa. The deformation capacity of structural concrete elements is an important aspect in the design of such structures. It mainly depends on the ductility of the reinforcement. Therefore, ductility of the reinforcement is as essential to structural concrete as its strength.

Reinforcing steel is generally assumed as elastic-plastic for design calculations and f_{sy} is taken to be the material strength, where the stress-strain curve is assumed horizontal when f_{sy} is reached. Under service loads steel stress is less than yield

stress and its behavior is linear-elastic; the stress-strain curve in compression is also assumed to be similar to that in tension.

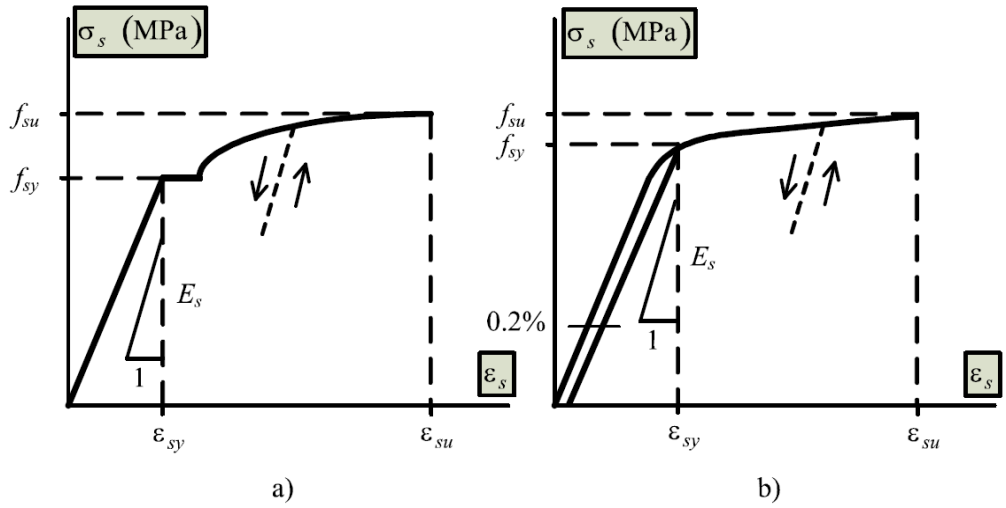

Figure 2-3 Stress-strain characteristics of reinforcement in uniaxial tension: a) hot-rolled, heat-treated, low-carbon steel; b) cold-worked or high-carbon steel

2.1.4 Steel-Concrete bond

The bond between steel and concrete has three main components: chemical adhesion, friction and mechanical interlock. Chemical adhesion is the original bond developed between concrete and steel before any slip occurs. The effect of chemical adhesion is very small and it does not allow any slip. As the steel bar is loaded up to a certain level, chemical adhesion bond cannot provide sufficient bond force and breaks down. As soon as the chemical bond fails, relative movement can occur between concrete and steel. As one of the components of bond force, friction comes into play. The radial forces around the steel bar can create a certain amount of friction forces counteracting the slip effect. Also, mechanical interlock, which is created by the ribs on the bar embedded in the concrete, becomes the most important component as illustrated in Figure 2-4. As the load continuous to increase, the steel bar is elongated more significantly. Poisson's ratio's effect causes the cross section to decrease. The radial forces are significantly reduced due to that effect, so friction becomes negligible at this stage and leaving the bearing of concrete becomes the primary force transfer mechanism. Cracks begin to form adjacent to steel rebar.

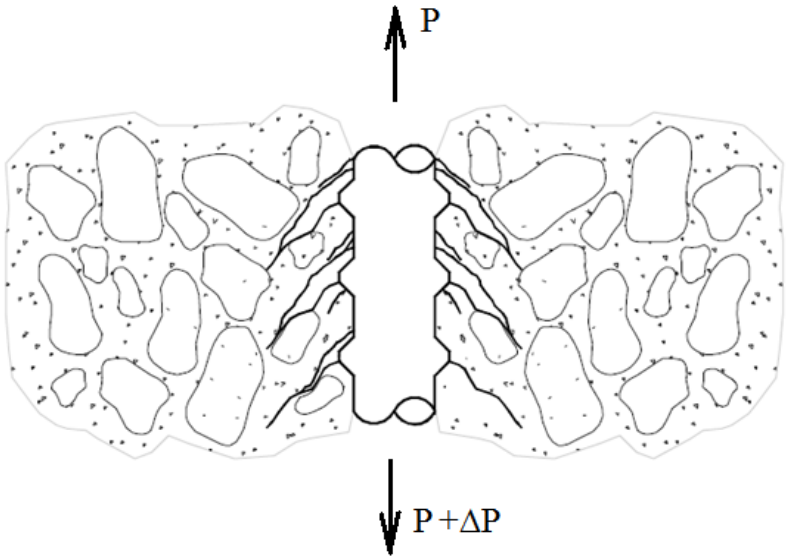

Figure 2-4 Steel-concrete bond

2.1.5 Tension-stiffening

A comprehensive literature review on tension-stiffening models and deformation behavior of RC members has been performed by Kaklauskas (2001) and Gribniak (2009).

The first studies which defined the behavior of concrete under tensile stress began towards the end of 19th century when, though the intense activity of skillful builders, the technique of RC reached certain stages that were fundamental for its subsequent success. Joly (1898a, 1898b) and Considere (1899a, 1899b) who made a decisive contribution to explaining the behavior of RC flexural and tensile members performed first intuitions on the tension-stiffening. After the response of the elements to the applied actions had been explained, its behavior as defined though mathematical models, necessary for the calculation theories according to Albenga (1945), were many and contradictory.

Cracking in a reinforced concrete member also causes a significant increase in deflection. This is a result of the reduction of bending stiffness at cracked section when the effect of tensile concrete below the neutral axis diminishes. However, at the sections between successive cracks, some tensile stress is restrained in the concrete around steel bars due to the actions of bond, contributing to the bending stiffness of the member. This is called tension-stiffening effect. If the tension-stiffening effect is neglected, calculated deflection may be overestimated by a large proportion. In simplified methods of deflection calculation the tension-stiffening

effect is incorporated in a semi empirical manner by using the effective moment of inertia method. In analytical methods, the deflection is calculated using curvature values, evaluated by adopting a non-linear stress-strain relationship for tensile concrete. This allows concrete to retain some tensile stress beyond the cracking strain.

Many theoretical models of RC in tension have been proposed to predict cracking and deformations of RC members. Generally, these models may be separated into three main approaches:

- Average stress-average strain: simple approaches, extensively used in numerical analyses, based on smeared crack model.
- Bond stress transfer in the interface zone of concrete and reinforcement and fracture mechanics: these approaches aim at modeling bond between concrete and reinforcement steel and use the fracture mechanics principles to predict cracking behavior of RC elements.
- Analytical-empirical: the earliest approaches were developed based on the analysis of test data. Such simplified calculation techniques are broadly presented in the design codes. The techniques on this approach in more detail are presented in Section 2.3.

2.1.5.1 Average Stress- Average Strain

This simple approach, extensively applied in numerical analyses, is based on use of average stress-strain tension-stiffening relationship. The approach introduced by Rashid (1968) is based on smeared crack model, i.e. cracks are smeared out in the continuous fashion and the cracked concrete is assumed to remain a continuum. Concrete becomes orthotropic with one of the material axes being oriented along the direction of cracking.

Differently from the discrete crack model, which is tracing individual cracks, smeared crack model deals with average strains and stresses This model can handle single, multiple and distributed cracks in a unified manner. Thus, it can be used for both plain concrete and RC structures (Cervenka 1995). In FE analysis, smeared crack model has proven to be more flexible and more computationally effective concerning the discrete crack model since no topological constraints exist.

Tension-stiffening can be attributed either to tensile reinforcement (steel related model) or to concrete (concrete-related model). In the latter approach, it may be

assumed that tension-stiffening is effective either in the whole tension area or in the specified zone (close to reinforcement), called the effective area.

Gilbert & Warner (1978), and others have used the steel related approach. It should be noted that this approach is relatively rarely applied.

In the effective area approach, the influence of tension-stiffening is limited to a volume of concrete in relatively close proximity to the bar (tension stiffening zone). In Model Code 90 (CEB-FIP 1991) tension-stiffening zone was limited to concrete area within 7.5 bar diameters from the reinforcement. Outside this zone, the second mechanism of post cracking prevails, that of tension softening (Vecchio & Collins 1986, Stramandinoli & Rovere 2008).

2.1.5.2 Bond Stress Transfer in the Interface Zone of Concrete and Reinforcement and Fracture Mechanics

This approach is based on bond-slip relationship, which models the bond-action between concrete and reinforcement. Saliger (1936) was the first one, who has published the basis for all theories using this approach. The bond-action at the interface of steel bars and surrounding concrete has great influence on the initiation and propagation of cracks in RC members. The bond-action is the main contributing factor to the tension-stiffening effect in concrete structures. In a cracked RC member, an increase in loading will result in an increase in steel strain, causing an extension of the reinforcing bar. Consequently, ribs in the bar will tend to move towards the nearest crack relative to the surrounding concrete, i.e. bond-slip is initialised. This will increase the rib bearing stress on concrete, contributing to the bondslip.

2.2 Finite Element Method

In recent years, numerical techniques have been rapidly progressing for decades and now offer very powerful and general analytical tool for analysis of RC structures, such commercial softwares include (*ABAQUS*, *DIANA*, *ATENA*, ANSYS etc). In FE approach, tension-stiffening effect and consequently deflection can be predicted rationally

Concrete models in *ATENA* software (Cervenka 1985, Cervenka *et al*. 2002) are based on smeared crack concept and damage approach. Concrete without cracks is considered as an isotropic material and concrete with cracks as an orthotropic

material. In the fixed crack model crack direction and material axes are defined by the principal stress direction at the onset of cracking when the principal stress exceeds the tensile strength. In further analysis, this direction is fixed and cannot be changed though direction of principal strains may vary. A rotation of principal strain axes generates a shear stress on the crack plane. Consequently, the model of shear in cracked concrete becomes important. In the model a variable shear retention factor according to Kolmar (1986) is used, in which the shear modulus on the crack plane reduces with the crack opening.

It should be noted that the tension-stiffening effect is not explicitly included as a constitutive law in the above model. However, the fracture mechanics based model reaches almost the same effect, where distinct cracks formed and a contribution of concrete between cracks generates a tension-stiffening effect, as was shown by Cervenka (2002). Of course, this model has its limits bound to numerical discretization and is objective only for sufficiently fine mesh sizes.

2.3 Design Code Method

This section briefly overviews deflection calculation methods for short term loading from the two well-known design codes: Eurocode 2 [2], and ACI 318[1]. An elaborate description of these two code methods discussed in section 3.2 and 3.3 respectively.

2.3.1 Eurocode 2

The deflection calculations in the European structural concrete codes, Eurocode 2 (CEN 1992) [2] and BS 8110-2 (BS 1985), are based on the determination of the curvatures and deflections of concrete beam corresponding to its uncracked and fully-cracked conditions. In Eurocode 2 model, a reinforced concrete member is divided into two regions: region I, uncracked and region II, fully cracked. In region I, both the concrete and steel behave elastically, while in region II the reinforcing steel carries all the tensile force on the member after cracking. The average curvature is expressed as:

$$\alpha = (1-\zeta)\alpha_I + \zeta\alpha_{II} \qquad \textbf{Equation 2-1}$$

Here α_I and α_{II} are curvatures calculated for the uncracked and fully cracked regions respectively; ζ is a distribution coefficient (allowing for tension-stiffening at a section) given by:

$$\zeta = 1 - \beta\left[\frac{\sigma_{sr}}{\sigma_s}\right]^2 \qquad \textbf{Equation 2-2}$$

Here β is a coefficient taking into account the influence of duration of the loading or repeated loading on the average strain (β=1.0 for a single short-term loading and β=0.5 for sustained loads or many cycles of repeated loading); ζ=0 for uncracked sections; σ_s is the stress in the tensile reinforcement calculated on the basis of a cracked section; σsr is the stress in the tensile reinforcement calculated on the basis of a cracked section under the loading conditions causing first cracking. Note that ratio σ_{sr}/σ_s may be replaced by Mcr/M for flexure or Ncr/N for pure tension, where M_{cr} is the cracking moment and N_{cr} is the cracking force.

The calculation of α_I and α_{II} may be obtained from the relation:

$$\alpha_I = \frac{M}{EI_I} \text{ or } \alpha_{II} = \frac{M}{EI_{II}} \qquad \textbf{Equation 2-3}$$

The code states "it is known that actual deformations may considerably differ from calculated values, due to the dispersion of the material properties, the environmental effects, the influence of loading stages or restraint conditions at the supports. Different models may be used for the calculation of deformations, depending on the degree of accuracy required. For practical purposes, in order to prevent the occurrence of damage due to deformations, a rough estimate of displacements will often be sufficient." This clearly states that other models can be used to model deflections of reinforced concrete members.

The code uses the concept of averaging the flexibilities of the uncracked and cracked portions of the beam rather than averaging the stiffness. The tension-stiffening model setting the stage for equation 2-1 is presented in CEB-FIP Model Code (CEB 1990), where the application of the model to axial response of reinforced concrete tension member is depicted.

2.3.2 American Code (ACI 318)

The short-term deflection calculation procedure is described by following.

Uncracked members - gross moment of inertia I_g - when the maximum flexural moment at service load in a beam or a slab causes a tensile stress less than the modulus of rupture, f_r no flexural tension cracks develop at the tension side of the concrete element if the member is not restrained or the shrinkage and temperature tensile stresses are negligible. In such a case, the effective moment of inertia of the

uncracked transformed section, II, is applicable for deflection computations. However, for design purposes, the gross moment of inertia, I_g, neglecting the reinforcement contribution, can be used with negligible loss of accuracy. The combination of service loads with shrinkage and temperature effects due to end restraint may cause cracking if the tensile stress in the concrete exceeds the modulus of rupture.

The elastic deflection for non-cracked members can thus be expressed in the following general form:

$$\delta = s\frac{wl^4}{E_c I_e} \qquad \textbf{Equation 2-4}$$

Here "s" is a factor that depends on support fixity and loading conditions; M is the maximum flexural moment along the span and E_c is the modulus of elasticity of concrete.

Cracked members - effective moment of inertia I_e - tension cracks occur when the imposed loads because bending moments in excess of the cracking moment, thus resulting in tensile stresses in the concrete which are higher than its modulus of rupture. The cracking moment, M_{cr} may be computed as follows;

$$M_{cr} = \frac{f_r I_g}{y_t} \qquad \textbf{Equation 2-5}$$

2.4 Other Methods

In general, the displacements are determined by integration of curvatures, setting the boundary conditions. In that case, we assume the mean curvature for the zone subjected to cracking and the section curvature for the uncracked zones. Having determined both mean curvature and axial deformation along the axis or in the sections into which the structure has been subdivided, the calculation of displacements is only a geometrical problem which can be solved in various ways.

2.4.1 Branson's Method

In this method which use and effective constant moment of inertia originally proposed by Branson (1965, 1977) [6]. This empirical relationship is given by Equation 2-5 and represents a gradual transition from the uncracked transformed moment of inertia (I_{unc}) to a fully cracked moment of inertia (I_{crd}) based on a cracked transformed section analysis. The intent of this equation is to account for the effects of reinforcement and cracking on member stiffness under increasing load. I_{unc} is

replaced by the gross moment of inertia (I_g) in most cases, except for heavily reinforced sections. Use of I_{cr} implies that behavior at a cracked section is linear elastic up to yielding of the steel reinforcement.

$$I_e = \left(\frac{M_{cr}}{M_a}\right)^m I_g + \left[1 - \left(\frac{M_{cr}}{M_a}\right)^m\right] I_{cr} \qquad \textbf{Equation 2-6}$$

The cracking moment M_{cr} is determined from the elastic flexure formula; and M_a represents the applied service load moment at which deflection is being calculated. Setting the power m equal to 4 accounts for the tensile contribution of concrete between cracks, referred to as tension stiffening, and gives an effective stiffness at the section only. An average stiffness over the entire span is obtained by using a value of 3 for m, in order to reflect the change in member stiffness (EI) along the length of beam in addition to the tension stiffening effect of concrete. ACI 318-02 set the value of m to 3 as it will be discussed in section 3.3.

2.4.2 Bischoff's Method

Bischoff [5], revaluated Bronson's original equation for I_e, and determines that the accuracy of Equation 2.5 is affected by the ratio I_g / I_{cr}. The tension stiffening effect in Equation 2.5 is highly dependent on both the power m and ratio I_g / I_{cr}, and is overestimated for values of $I_g / I_{cr} > 3$ when m equals 3. The ratio I_g / I_{cr} in turn depends on the reinforcing ratio r as well as the modular ratio n. Reasonable values of Ie are only obtained for steel reinforced concrete beams when $\rho > 1\%$ since this corresponds to a ratio of

$I_g / I_{cr} < 3$.

He then stated that Branson's equation gives a weighted average of the gross and cracked moments of inertia at a given load level. However, tension stiffening really represents a variation in stiffness of uncracked and cracked sections along the length of member. This is analogous to a series of cracked and uncracked springs (Farra and Jaccoud 1992) where the average or effective stiffness is then determined by taking a weighted average of the inverse stiffness values, that is 1/(EI) and not EI. Given that the effective member response is also being calculated at a specified level of load, then deflection and not inertia needs to be averaged. Deflection is inversely proportional to the moment of inertia. Hence, a weighted average should be taken of the inversed moment of inertia, leading to a subtle change in Equation 2.5 that is given below.

$$\frac{1}{I_e}=\left(\frac{M_{cr}}{M_a}\right)^m\frac{1}{I_g}+\left[1-\left(\frac{M_{cr}}{M_a}\right)^m\right]\frac{1}{I_{cr}}\geq\frac{1}{I_g}$$ **Equation 2-7**

Calibration of this equation with Branson's original equation [using m=3 in Equation 2.5] for a beam with I_g / I_{cr}=2.2 now gives m=2.

2.4.2.1 Comparison between Branson's and Bischoff's Method

To explain the differences between the effective moment of inertia expressions proposed by Branson (1965) and Bischoff (2005), Bischoff and Scanlon (2007) and Bischoff (2007) used spring models (Fig. 1). Accordingly, Branson's approach models the uncracked and cracked portions of a concrete beam as springs in parallel, while Bischoff's approach models them as springs in series. In the springs-in-parallel model (Fig. 1b) the stiffnesses of the uncracked and cracked portions are averaged, while in springs-in-series model the flexibilities are averaged. The tension-stiffening approach used by Bischoff (2005) indicates that the weighted flexibilities of the uncracked and cracked portions should be averaged to obtain the overall material response of a cracked concrete beam. A cracked portion and an uncracked portion of a concrete beam, neighboring each other, resist approximately the same bending moment and their curvatures are integrated when assessing the deflections of the member. Consequently, the springs-in-series model used in Bischoff's approach represents the in-plane bending behavior of a cracked reinforced concrete beam more appropriately.

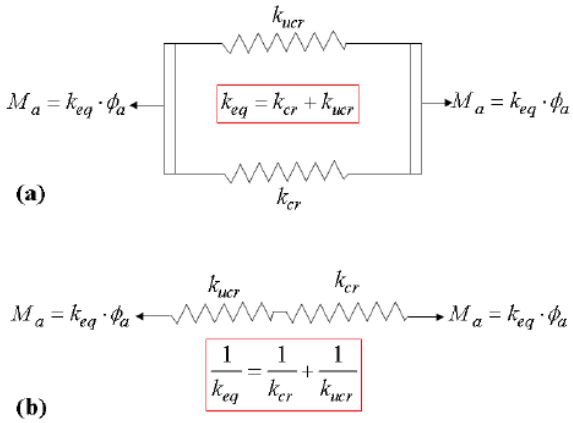

Figure 2-5 Spring Model for (a) Branson's effective moment of inertia; (b) Bischoff's effective moment of inertia [7]

3. Short-term Deformation of Flexural RC Beams-Theoretical Background

3.1 Load versus Deflection Response

The short-term or instantaneous deformation of a reinforced concrete cross-section subjected to combined bending and axial force can be readily determined using simple Modular Ratio Theory. After cracking, the properties of both the fully-cracked section and the uncracked section are often combined empirically to model tension stiffening and to approximate the average properties of the cracked region.

Consider the load-deflection response of a simply-supported, singly reinforced concrete beam or one-way slab shown in Figure 3-1. At loads less than the cracking load, P_{cr}, the member is uncracked and behaves homogeneously and elastically, and the slope of the load deflection plot is proportional to the second moment of area of the uncracked transformed section, I_{uncr}. The member first cracks at P_{cr} when the extreme fiber tensile stress in the concrete at the section of maximum moment reaches the flexural tensile strength of the concrete, $f_{ct,f}$. There is a sudden change in the local stiffness at and immediately adjacent to this first crack. On the section containing the crack, the flexural stiffness drops significantly, but the rest of the member remains uncracked. As load increases, more cracks form and the average flexural stiffness of the entire member decreases. If the tensile concrete in the cracked regions of the beam carried no stress, the load-deflection relationship would follow the dashed line ACD. If the average extreme fiber tensile stress in the concrete remained at $f_{ct,f}$ after cracking, the load-deflection relationship would follow the dashed line AE. In reality, the actual response lies between these extremes and is shown in Figure 1 as the solid line AB. The difference between the actual response and the zero tension response is the tension stiffening effect (which reduces the instantaneous deflection by 8£1, as shown in Figure 3-1).

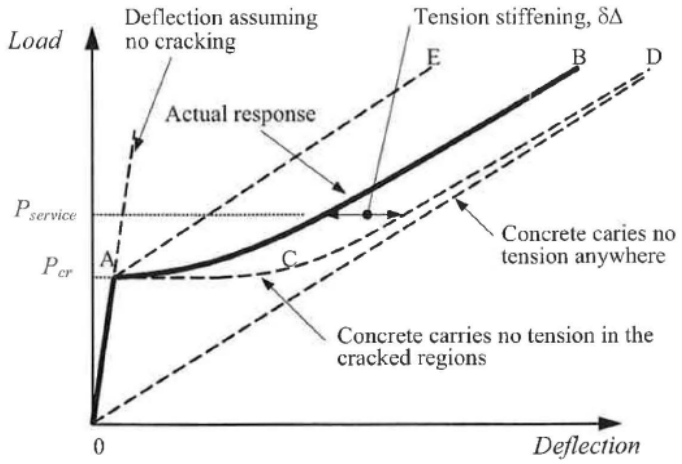

Figure 3-1 Typical load versus deflection relationship [4]

Tension stiffening is the contribution to the post-cracking stiffness of the member of the intact tensile concrete between the cracks. At each crack, the tensile concrete carries no stress, but as the distance from the crack increases, the tensile stress in the concrete increases due to the bond between the tensile concrete and the tensile reinforcement. As the load increases, the average tensile stress in the concrete reduces as more cracks develop and the actual response becomes approximately parallel to the no tension response (as shown in Figure 3-1), when the crack pattern is fully developed and the number of cracks has stabilized. For slabs containing small quantities of tensile reinforcement (typically $A_{st}/bd < 0.005$), tension stiffening may be responsible for more than 50% of the stiffness of the cracked member at service loads and δΔ remains significant up to an beyond the point where the steel yields and the ultimate load is approached.

The keys to predicting the instantaneous deflection are first to evaluate the load required to cause first cracking or, more precisely, the moment to cause first cracking at the critical cross-section, and secondly to model tension stiffening accurately. Both these tasks are not straightforward. Restraint to shrinkage provided by the bonded reinforcement and restraint to shrinkage at the member's ends can cause significant tension in the concrete in the first few days after casting. Cracking may therefore occur at loads far less than that required to produce an extreme fiber tensile stress equal to the modulus f rupture, $f_{ct,f}$; in a member without shrinkage.

3.2 Calculation of Short Term Deflection in Accordance to EC-2

The short term deflection of a 7.0m span simply supported beam whose section is shown in Figure 3-2. The beam supports the interior floor spans of an office building.

Deflections will be calculated using the rigorous method given in EC2, together with an alternative simplified method. The results will then be compared with the limiting span/effective depth ratios given in EC2.

3.2.1 Design data

Span = 7.0 m

G_k = 18.75 kN/m

Q_k = 15 kN/m

A'_s = 402 mm^2 ($2\phi16$)

A_s = 1810 mm^2 ($4\phi24$)

f_{ck} = 25 N/mm^2 (concrete strength class C25/30)

f_{yk} = 500N/mm^2 (Steel B500B)

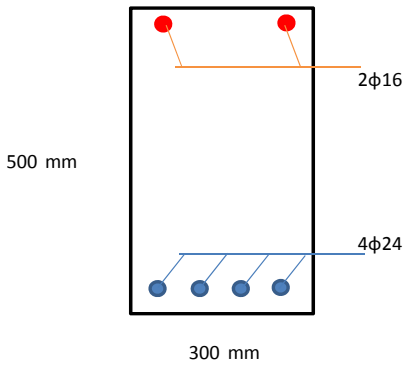

Figure 3-2 Cross-Section

3.2.2 Calculation Method

The requirements for the calculation of deflections are given in Section 7.4.3 and Appendix C of EC2.

Two limiting conditions are assumed to exist for the deformation of concrete sections

1) Uncracked

2) Cracked.

Members which are not expected to be loaded above the level which would cause the tensile strength of the concrete to be exceeded, anywhere in the member, will be considered to be uncracked. Members which are expected to crack will behave in a manner intermediate between the uncracked and fully cracked conditions.

For members subjected dominantly to flexure, the Code gives a general equation for obtaining the intermediate value of any parameter between the limiting conditions

$$\alpha = (1-\zeta)\alpha_I + \zeta\alpha_{II}$$ **Equation 3-1**

Where

α is the parameter being considered

α_I and α_{II} are the values of the parameter calculated for the uncracked and fully cracked conditions respectively

ζ is a distribution coefficient (allwing for tension sttifening at a section) given by

$$\zeta = 1 - \beta\left[\frac{\sigma_{sr}}{\sigma_s}\right]^2 \qquad \textbf{Equation 3-2}$$

$\zeta = 0$ for uncracked sections

β is a coefficent taking account of the influence of the duration of the loading or of the repeated loading on the average strain

=1.0 for a single short-term loading

= 0.5 for sustained loads or many cycles of repeated loading

σ_s is the stress in the tension reinforcemnt calculated on the basisi of cracked section

σ_{sr} is the stress in the tension reinforcemnt calculated on the basis of cracked section under the loading conditions causing first craking

Note: σ_{sr}/σ_s may be replaced by M_{cr}/M for flexure or N_{cr}/N for pure tension, where M_{cr} is the cracking moment and N_{cr} is the cracking force.

The effects of creep are catered for by the use of an effective modulus of elasticity for the concrete given by

$$E_{c,eff} = \left[\frac{E_{cm}}{1+\varphi(\infty, t_o)}\right] \qquad \textbf{Equation 3-3}$$

Where:

$\varphi(\infty, t_o)$ is the creep coefficent relevant for the load and time interval

Curvatures due to shrinkage may be assessed from

$$\frac{1}{r_{cs}} = \varepsilon_{cs}\alpha_e\frac{S}{I} \qquad \textbf{Equation 3-4}$$

Where:

$1/r_{cs}$ is the curvature due to shrinkage

ε_{cs} is the free shrinkage strain

S is the first moment of area of the reinforcemnt about the centroid of the section

I second moment of area of the section

α_e is the effective modular ratio

Shrinkage curvatures should be calculated for the uncracked and fully cracked conditions and the final curvature assessed by use of Equation 1.1

- ✓ FOR THIS CALCULATION THE EFFECT OF SHRINKAGE AND CREEP ARE IGNORED!

In accordance with the Code, the rigorous method of assessing deflections is to calculate the curvatures at frequent sections along the member and calculate the deflections by numerical integration.

The simplified approach, suggested by the Code, is to calculate the deflection assuming firstly the whole member to be uncracked and secondly the whole member to be cracked. Equation 1.1 is used to assess the final deflection,

3.2.3 Rigorous Assessment

The procedure is, at frequent intervals along the member, to calculate

1) Moments
2) Curvatures
3) Deflections.

Here, calculations will be carried out at the mid-span position only, to illustrate this procedure, with values at other positions along the span being tabulated there after.

3.2.3.1 Calculation of Moments

For buildings, it will normally be satisfactory to consider the deflections under the quasi-permanent combination of loading, assuming this load to be of long duration.

The quasi-permanent combination of loading is given, for one variable action, by

$G_k + \psi_2 Q_k$

$\psi_2 = 0.3$

Therefore

$Loading = 18.75 + (0.3 \times 15) = 23.25 kN/m$

$$\text{Mid-Span bending moment (M)} = \frac{23.25 \times 7^2}{8} = 142.41 kNm$$

3.2.3.2 Calculation of Curvatures

In order to calculate the curvatures it is first necessary to calculate the properties of the uncracked and cracked sections and determine the moment at which cracking will occur.

3.2.3.2.1 Flexural Curvature

The effective modulus of elasticity ($E_{c,eff}$) = $\frac{E_{cm}}{1+\phi}$

For concrete strength class C25/30, E_{cm} = 31kN/mm^2

As stated above creep is ignored:- $E_{c,eff} = E_{cm}$ = 31kN/mm^2 efective modular ratio (α_e) = $\frac{E_s}{E_{c,eff}}$

Modulus of elasticity of reinforcemnt (E_s) = 200kN/mm^2 [EC2, section 3.2.7.4]

Therefore

$$\alpha_e = \frac{200}{31} = 6.45$$

$$\rho = \frac{A_s}{bd} = \frac{1810}{300 \times 455} = 1.326 \times 10^{-2}$$

$$\rho' = \frac{A'_s}{bd} = \frac{402}{300 \times 455} = 2.919 \times 10^{-3}$$

I. UNCKRACKED CROSS-SECTION

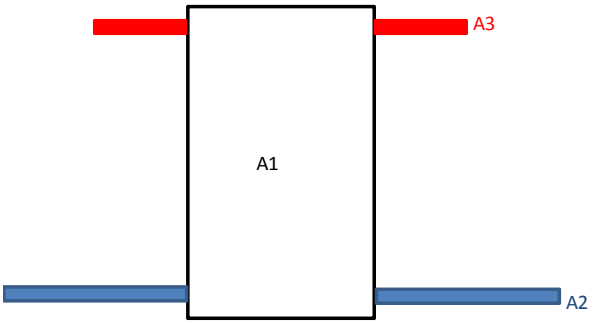

Figure 3-3 Equivalent transformed cross section

Neutral axis depth of the uncracked section:

$A_1 = b \times h = 300x500 = 150000mm^2$

$A_2 = (\alpha_e - 1) \times A_s = (6.45 - 1) \times 1810 = 9864.5mm^2$

$A_3 = (\alpha_e - 1) \times A'_s = (6.45 - 1) \times 402 = 2190.9mm^2$

And considering the top fiber as a refrecnce axis

$x_1 = \frac{h}{2} = 250mm$

$x_2 = d = 455mm$

$x_3 = d' = 41mm$

Therefore:-

$$x = \frac{(A_1 \times x_1) + (A_2 \times x_2) + (A_3 \times x_3)}{(A_1 + A_2 + A_3)} = 259.65mm$$

The second moment of the area of the uncracked section

$$I_1 = \left(\frac{bh^3}{12}\right) = \left(\frac{300 \times 500^3}{12}\right) = 3125000000mm^4$$

$I_2 \approx 0$

$I_3 \approx 0$

$A_1 = b \times h = 300x500 = 150000mm^2$

$A_2 = (\alpha_e - 1) \times A_s = (6.45 - 1) \times 1810 = 9864.5mm^2$

$A_3 = (\alpha_e - 1) \times A'_s = (6.45 - 1) \times 402 = 2190.9mm^2$

$y_1 = x - \frac{h}{2} = 259.65 - 250 = 9.65mm$

$y_2 = d - x = 455 - 259.65 = 195.35mm$

$y_3 = x - d' = 259.65 - 41 = 218.65mm$

Therefore : -

$$I_I = I_1 + I_2 + I_3 + (A_1 \times y_1^2) + (A_2 \times y_2^2) + (A_3 \times y_3^2)$$

$$I_I = 3125000000 + 0 + 0 + (150000 \times 9.65^2) + (9864.5 \times 195.35^2) + (2190.9 \times 218.65^2)$$

$$I_I = 3620155858.4665mm^4$$

II. CRACKED CROSS-SECTION

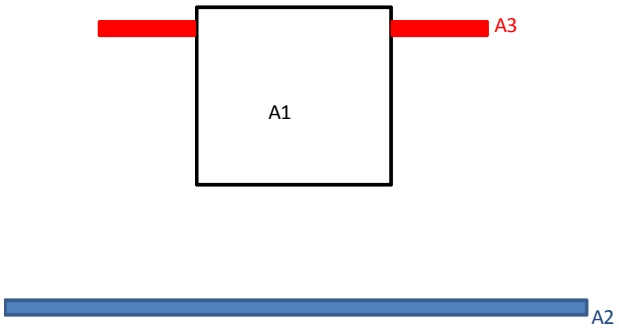

Figure 3-4 Equivalent transformed cracked cross section

Neutral axis depth of the cracked section: The position of the neutral axis can be determined by taking the static moments of the shaded areas (Figure 3-4), about the centroidal axis (same as neutral axis):

$$\frac{1}{2}b(k_x d)^2 + (\alpha_e - 1)A'_s(k_x d - d') = \alpha_e A_s(d - k_x d)$$

Dividing the above expression by bd^2 and denoting $\rho = A_s/bd$ and $\rho' = A_s/bd$ results in:

$$k_x = \frac{x}{d} = -[\alpha_e\rho + (\alpha_e - 1)\rho'] + \sqrt{[\alpha_e\rho + (\alpha_e - 1)\rho']^2 + 2[\alpha_e\rho + (\alpha_e - 1)\rho'\frac{d'}{d}}$$

$x = 0.327d = 149.1004mm$

The second moment of the area of the cracked section

$$I_1 = \left(\frac{bh^3}{12}\right) = \left(\frac{300 \times 149.1004^3}{12}\right) = 82865969.19mm^4$$

$I_2 \approx 0$

$I_3 \approx 0$

$A_1 = b \times h = 300x149.1004 = 44730.11244mm^2$

$A_2 = \alpha_e \times A_s = 6.45 \times 1810 = 11668.64516mm^2$

$A_3 = (\alpha_e - 1) \times A'_s = (6.45 - 1) \times 402 = 2191.112258mm^2$

$$y_1 = x - \frac{x}{2} = \frac{149.1004}{2} = 74.55019mm$$

$y_2 = d - x = 455 - 149.1004 = 305.8996mm$

$y_3 = x - d' = 149.1004 - 41 = 108.1004mm$

Therefore : -

$$I_{II} = I_1 + I_2 + I_3 + (A_1 \times y_1^2) + (A_2 \times y_2^2) + (A_3 \times y_3^2)$$

$$I_{II} = 1448957116mm^4$$

III. CRACKING MOMENT

$$M_{cr} = \frac{f_{ctm} I_I}{y_t}$$

$y_t = h - x = 500 - 259.65 = 240.35$

For concrete strength grade C25/30, $f_{ctm} = 2.6N/mm^2$

Therefore

$$M_{cr} = \frac{2.6 \times 3620155858.4665}{240.35} = 39.2kNm$$

The section has cracked, since

$$M_{cr} < M = 142.14kNm$$

IV. CURVATURE OF THE UNCRACKED SECTION

$$\frac{1}{r_I} = \frac{M}{E_{c,eff} I_I} = \frac{142.41 \times 10^6}{31 \times 10^3 \times 3620155858.4665} = 1.27 \times 10^{-6} rad / mm$$

V. CURVATURE OF THE CRACKED SECTION

$$\frac{1}{r_{II}} = \frac{M}{E_{c,eff} I_{II}} = \frac{142.41 \times 10^6}{31 \times 10^3 \times 1448957116} = 3.1704671705 \times 10^{-6} rad / mm$$

VI. INTERMIDIATE CURVATURE VALUE

Having obtained the values for the two limiting conditions Equation 1.1s used to assess the intermediate value

$$\frac{1}{r} = (1-\zeta)\frac{1}{r_I} + \zeta\frac{1}{r_{II}}$$

$$\zeta = 1-\beta\left[\frac{\sigma_{sr}}{\sigma_s}\right]^2 = \zeta = 1-\beta\left[\frac{M_{cr}}{M}\right]^2$$

$\beta = 1.0$ for single short term loading

$$\frac{M_{cr}}{M} = \frac{39.2}{142.41} = 0.275$$

$$\zeta = 1-1\times 0.275^2 = 0.924$$

$$\frac{1}{r} = (1-0.924)\times 1.27\times 10^{-6} + 0.924\times 3.1704671705\times 10^{-6} = 3.02647080419\times 10^{-6}\, rad/mm$$

3.2.3.2.2 *Shrinkage curvature*

Here the effect of shrinkage is ignored as that of creep.

3.2.3.2.3 *Total curvature*

Here below is the tabulated result for curvature along the span on the beam

Table 3-1 Total curvature in accordance to EC2

X/l	Moment[kNm]	$1/r_I$ [x10^{-6}rad/mm]	$1/r_{II}$ [x10^{-6}rad/mm]	ζ	1/r [x10^{-6}rad/mm]	$1/r_{cs}$ [x10^{-6}rad/mm]	$1/r_{tot}$ [x10^{-6}rad/mm]
0.000	0.000	0.000	0.000	0.000	0.000	0.000	0.000
0.100	51.266	0.457	1.141	0.415	0.741	0.000	0.741
0.200	91.140	0.812	2.029	0.815	1.804	0.000	1.804
0.300	119.621	1.066	2.663	0.893	2.492	0.000	2.492
0.400	136.710	1.218	3.044	0.918	2.893	0.000	2.893
0.500	142.406	1.269	3.170	0.924	3.026	0.000	3.026
0.600	136.710	1.218	3.044	0.918	2.893	0.000	2.893
0.700	119.621	1.066	2.663	0.893	2.492	0.000	2.492
0.800	91.140	0.812	2.029	0.815	1.804	0.000	1.804
0.900	51.266	0.457	1.141	0.415	0.741	0.000	0.741
1.000	0.000	0.000	0.000	0.000	0.000	0.000	0.000

3.2.3.3 *Calculation of Deflection*

Having calculated the total curvatures, the deflections may be calculated by numerical integration using the trapezoidal rule.

The uncorrected rotation at any point may be obtained by the first integral given by

$$\theta_x = \theta_{x-1} + \left(\frac{\frac{1}{r_x} + \frac{1}{r_{x-1}}}{2}\right)\times\frac{l}{n} \qquad \textbf{Equation 3-5}$$

Having calculated the uncorrected rotations, the uncorrected deflections may be obtained by the second integral given by:

$$\delta_x = \delta_{x-1} + \left(\frac{\theta_x + \theta_{x-1}}{2} \right) \times \frac{l}{n}$$ **Equation 3-6**

Where: the subscript x denotes the values of the parameters at the fraction of the span being considered, and the subscript x-1 denotes the values of the parameters at the preceding fraction of the span.

L is the span

n is the number of the span divisions considered

Here the uncorrected rotatioin at 0.1*l*

$$\theta_{0.1l} = \theta_0 + \left(\frac{\frac{1}{r_{0.1l}} + \frac{1}{r_0}}{2} \right) \times \frac{l}{n} = 0 + \left(\frac{0.741 + 0}{2} \right) \times 10^{-6} \times \frac{7000}{10} = 0.25935 \times 10^{-3} rad.$$

and the uncorrected deflection at 0.1*l*

$$\delta_{0.1l} = \delta_0 + \left(\frac{\theta_{0.1l} + \theta_0}{2} \right) \times \frac{l}{n} = 0 + \left(\frac{0.25935 + 0}{2} \right) \times 10^{-3} \times \frac{7000}{10} = 0.0907725 mm$$

The uncorrected deflections may then be corrected to comply with the boundary conditions of zero deflection at both supports. This is done by subtracting from the uncorrected deflections the value of the uncorrected deflection at the right hand support multiplied by the fraction of the span at the point being considered.

The values of the uncorrected rotations, uncorrected and corrected deflections at positions x/l along the span are given in Table 3-2.

Table 3-2 Deflections in accordance to EC2 [mm]

X/l	1st integral [10^{-3}rad]	2nd integral [mm]	Correction	Deflection
0.000	0.000	0.000	0.000	0.000
0.100	0.259	0.091	4.627	-4.536
0.200	1.150	0.584	9.254	-8.670
0.300	2.654	1.915	13.882	-11.966
0.400	4.538	4.433	18.509	-14.076
0.500	6.610	8.335	23.136	-14.801
0.600	8.682	13.687	27.763	-14.076
0.700	10.567	20.424	32.390	-11.966
0.800	12.070	28.347	37.018	-8.670
0.900	12.961	37.108	41.645	-4.536
1.000	13.221	46.272	46.272	0.000

3.3 Calculation of Short Term Deflection in Accordance to ACI-318

3.3.1 Design data

Span = 7.0 m

G_k = 18.75 kN/m

Q_k = 15 kN/m

A'_s = 402 mm^2 (2ϕ16)

A_s = 1810 mm^2 (4ϕ24)

f'_c = 25 N/mm^2

f_{yk} = 500N/mm^2

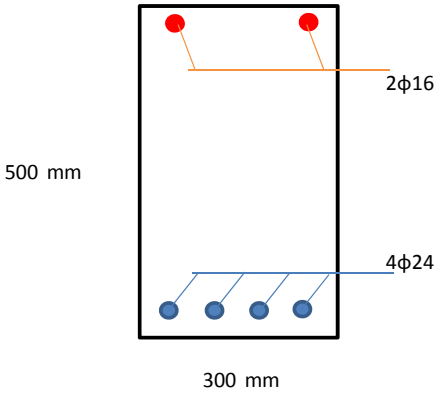

3.3.2 Calculation Method

The ACI 318 states “For calculation of immediate deflections of uncracked prismatic members, the usual methods or formulas for elastic deflections may be used with a constant value of E_cI_g along the length of the member. However, if the member is cracked at one or more sections, or if its depth varies along the span, a more exact calculation becomes necessary.

The ACI 318 technique is based on the method proposed by Branson, which uses the effective moment of inertia

$$I_e = \left(\frac{M_{cr}}{M_a}\right)^3 I_g + \left[1 - \left(\frac{M_{cr}}{M_a}\right)^3\right] I_{cr}$$ **Equation 3-7**

Here I_g is the moment of inertia for un-cracked concrete section ignoring reinforcement for simplicity; I_{cr} is the moment of inertia for the fully cracked section; M_a is the applied moment;

$$M_{cr} = \frac{f_r I_g}{y_t}$$

and

$$f_r = 7.5\lambda\sqrt{f'_c}$$

$$f_r = 0.623\lambda\sqrt{f'_c}\,(MPa)$$ is the modulus of rupture

y_t is the distance from the extreme tension fiber; f'_c is the specified compressive concrete cylindrical strength; factor λ for normal-weight concrete is assumed equal to 1.0.

3.3.3 Deflection Assessment

The procedure is, at frequent intervals along the member, to calculate

1) Moments
2) Deflections.

Here, calculations will be carried out at the mid-span position only, to illustrate this procedure, with values at other positions along the span being tabulated there after.

3.3.4 Calculation of Moments

Considering the same load combination to come up with the same load and hence check the method employed by the code in comparison to the Eurocode2.

The quasi-permanent combination of loading is given, for one variable action, by

$$G_k + \psi_2 Q_k$$

$$\psi_2 = 0.3$$

Therefore

$$Loading = 18.75 + (0.3 \times 15) = 23.25 kN/m$$

$$\text{Mid-Span bending moment (M)} = \frac{23.25 \times 7^2}{8} = 142.41 kNm$$

3.3.5 Calculation of Deflection

$E_c = 4500\sqrt{25} = 22.5 kN/mm^2$

Modulus of elasticity of reinforcemnt $(E_s) = 200 kN/mm^2$

Therefore

$$n = \frac{200}{22.5} = 8.89$$

Having calculated the moment, the deflections may be calculated by using the elastic deflection equation as follows:

$$\delta = \frac{5wl^4}{384E_c I_e}$$

I. UNCKRACKED CROSS-SECTION

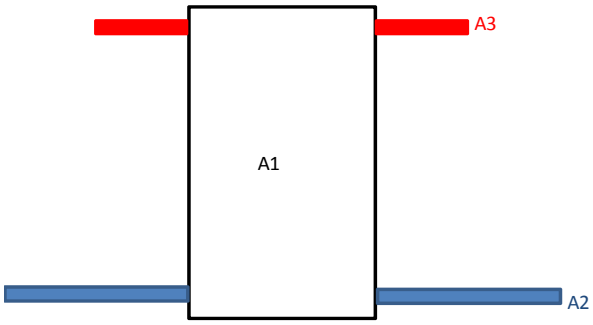

Figure 3-5 Equivalent transformed cross section

Neutral axis depth of the uncracked section:

$A_1 = b \times h = 300x500 = 150000mm^2$

$A_2 = (n-1) \times A_s = (8.89-1) \times 1810 = 14280.9mm^2$

$A_3 = (n-1) \times A'_s = (8.89-1) \times 402 = 3171.8mm^2$

And considering the top viber as a refrecnce axis

$x_1 = \frac{h}{2} = 250mm$

$x_2 = d = 455mm$

$x_3 = d' = 41mm$

Therefore:-

$$x = \frac{(A_1 \times x_1) + (A_2 \times x_2) + (A_3 \times x_3)}{(A_1 + A_2 + A_3)} = 263.52mm$$

The second moment of the area of the uncracked section

$$I_1 = \left(\frac{bh^3}{12}\right) = \left(\frac{300 \times 500^3}{12}\right) = 3125000000mm^4$$

$I_2 \approx 0$

$I_3 \approx 0$

$A_1 = b \times h = 300x500 = 150000mm^2$

$A_2 = (n-1) \times A_s = (8.89-1) \times 1810 = 14280.9mm^2$

$A_3 = (n-1) \times A'_s = (8.89-1) \times 402 = 3171.8mm^2$

$y_1 = x - \frac{h}{2} = 263.52 - 250 = 13.52mm$

$y_2 = d - x = 455 - 263.52 = 191.48mm$

$y_3 = x - d' = 263.52 - 41 = 222.52mm$

Therefore : -

$$I_I = I_1 + I_2 + I_3 + (A_1 \times y_1^2) + (A_2 \times y_2^2) + (A_3 \times y_3^2)$$

$$I_I = 3125000000 + 0 + 0 + (150000 \times 13.52^2) + (14280.9 \times 191.48^2) + (3171.8 \times 222.52^2)$$

$$I_I = 3833074063.08208mm^4$$

II. CRACKED CROSS-SECTION

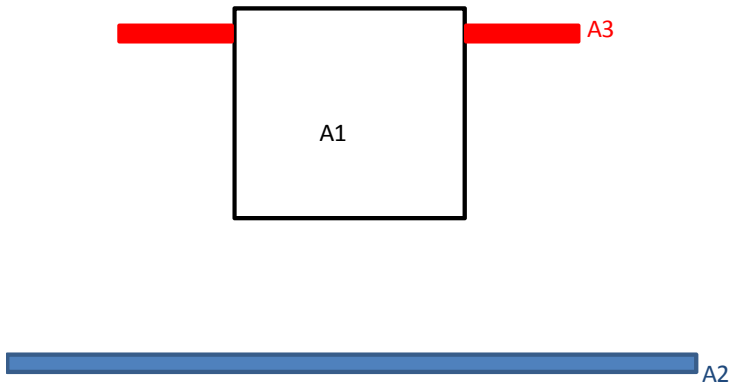

Figure 3-6 Equivalent transformed cracked cross section

Neutral axis depth of the cracked section:

$$\frac{1}{2}b(k_x d)^2 + (n-1)A'_s(k_x d - d') = nA_s(d - k_x d)$$

Dividing the above expression by bd^2 and denoting $\rho = A_s/bd$ and $\rho' = A_s/bd$ results in:

$$k_x = \frac{x}{d} = -[n\rho + (n-1)\rho'] + \sqrt{[n\rho + (n-1)\rho']^2 + 2[n\rho + (n-1)\rho'\frac{d'}{d}}$$

$x = 0.368d = 167.7308mm$

The second moment of the area of the cracked section

$$I_1 = \left(\frac{bh^3}{12}\right) = \left(\frac{300 \times 167.7308^3}{12}\right) = 117971943 mm^4$$

$I_2 \approx 0$

$I_3 \approx 0$

$A_1 = b \times h = 300x241.44 = 50319.25037 mm^2$

$A_2 = n \times A_s = 8.89 \times 1810 = 16076.8 mm^2$

$A_3 = (n-1) \times A'_s = (8.89-1) \times 402 = 3170.7022 mm^2$

$y_1 = x - \frac{x}{2} = \frac{167.7308}{2} = 83.86542 mm$

$y_2 = d - x = 455 - 167.7308 = 287.2692 mm$

$y_3 = x - d' = 167.7308 - 41 = 126.7308 mm$

Therefore : -

$I_{cr} = I_1 + I_2 + I_3 + (A_1 \times y_1^2) + (A_2 \times y_2^2) + (A_3 \times y_3^2)$

$I_{cr} = 1849526468 mm^4$

I. CRACKING MOMENT

Check if the section has cracked or not.

$$M_{cr} = \frac{f_r I_g}{y_t}$$

$f_r = 0.623\lambda\sqrt{f'_c}\,(MPa)$ is the modulus of rupture

$f_r = 0.623 \times 1.0 \times \sqrt{25} = 3.115 MPa$

$$M_{cr} = \frac{3.115 \times 3833074063.08208}{236.48} = 50.49 kNm$$

II. EFFECTIVE SECOND MOMENT OF THE AREA

$$I_e = \left(\frac{M_{cr}}{M_a}\right)^3 I_g + \left[1 - \left(\frac{M_{cr}}{M_a}\right)^3\right] I_{cr}$$

$$I_e = \left(\frac{50.49}{142.41}\right)^3 3833074063.08208 + \left[1 - \left(\frac{50.49}{142.41}\right)^3\right] 1849526468 = 1937923417.5848 mm^4$$

III. SHORTTERM DEFELECTION

$$\delta = \frac{5wl^4}{384 E_c I_e}$$

$$\delta = \frac{5 \times 23.25 \times 7000^4}{384 \times 22500 \times 1937923417.5848} = 16.67 mm$$

Table 3-3 Deflection in accordance to ACI

X/l	Moment [kNm]	I_e [mm^4]	δ [mm]
0.000	0.000	3833074063	0.000
0.100	51.266	3744329560	-2.708
0.200	91.140	2186760710	-8.774
0.300	119.621	1998680064	-13.143
0.400	136.710	1949447725	-15.781
0.500	142.406	1937930401	-16.670
0.600	136.710	1949447725	-15.781
0.700	119.621	1998680064	-13.143
0.800	91.140	2186760710	-8.774
0.900	51.266	3744329560	-2.708
1.000	0.000	3833074063	0.000

3.4 Calculation of Short Term Deflection in Accordance to ACI-318 with EC2 Material Property

3.4.1 Design data

Same design data is taken as in section 3.2.1.

3.4.2 Calculation Method

The same procedure is taken as in section 3.3 with the material property taken from EC 2. This is done to check whether the difference in the two codes approach is in the method or the material property.

3.4.3 Deflection Assessment

$G_k + \psi_2 Q_k$

$\psi_2 = 0.3$

Therefore

$Loading = 18.75 + (0.3 \times 15) = 23.25 kN/m$

$$\text{Mid-Span bending moment (M)} = \frac{23.25 \times 7^2}{8} = 142.41 kNm$$

3.4.4 Calculation of Deflection

$E_c = 4500\sqrt{25} = 22.5 kN/mm^2$

But $E_c = 31 N/mm^2$ is taken for the same reason stated above

Modulus of elasticity of reinforcemnt $(E_s) = 200 kN/mm^2$

Therefore

$$n = \frac{200}{31} = 6.45$$

III. UNCKRACKED CROSS-SECTION

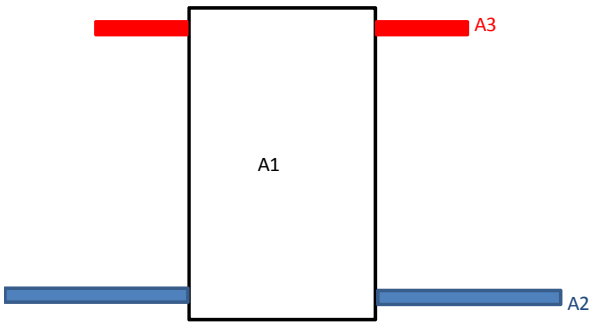

Figure 3-7 Equivalent transformed cross section

Neutral axis depth of the uncracked section:

$A_1 = b \times h = 300x500 = 150000mm^2$

$A_2 = (\alpha_e - 1) \times A_s = (6.45 - 1) \times 1810 = 9864.5mm^2$

$A_3 = (\alpha_e - 1) \times A'_s = (6.45 - 1) \times 402 = 2190.9mm^2$

And considering the top viber as a refrecnce axis

$x_1 = \frac{h}{2} = 250mm$

$x_2 = d = 455mm$

$x_3 = d' = 41mm$

Therefore:-

$$x = \frac{(A_1 \times x_1) + (A_2 \times x_2) + (A_3 \times x_3)}{(A_1 + A_2 + A_3)} = 259.65mm$$

The second moment of the area of the uncracked section

$$I_1 = \left(\frac{bh^3}{12}\right) = \left(\frac{300 \times 500^3}{12}\right) = 3125000000mm^4$$

$I_2 \approx 0$

$I_3 \approx 0$

$A_1 = b \times h = 300x500 = 150000mm^2$

$A_2 = (\alpha_e - 1) \times A_s = (6.45 - 1) \times 1810 = 9864.5mm^2$

$A_3 = (\alpha_e - 1) \times A'_s = (6.45 - 1) \times 402 = 2190.9mm^2$

$y_1 = x - \frac{h}{2} = 259.65 - 250 = 9.65mm$

$y_2 = d - x = 455 - 259.65 = 195.35mm$

$y_3 = x - d' = 259.65 - 41 = 218.65mm$

Therefore : -

$$I_I = I_1 + I_2 + I_3 + (A_1 \times y_1^2) + (A_2 \times y_2^2) + (A_3 \times y_3^2)$$

$$I_I = 3125000000 + 0 + 0 + (150000 \times 9.65^2) + (9864.5 \times 195.35^2) + (2190.9 \times 218.65^2)$$

$$I_I = 3620155858.4665mm^4$$

IV. CRACKED CROSS-SECTION

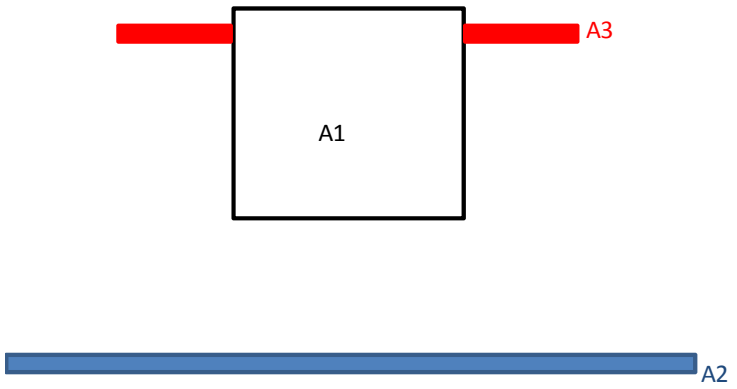

Figure 3-8 Equivalent transformed cracked cross section

Neutral axis depth of the cracked section:

$$\frac{1}{2} b (k_x d)^2 + (n-1) A'_s (k_x d - d') = n A_s (d - k_x d)$$

Dividing the above expression by bd^2 and denoting $\rho = A_s/bd$ and $\rho' = A_s/bd$ results in:

$$k_x = \frac{x}{d} = -[n\rho + (n-1)\rho'] + \sqrt{[n\rho + (n-1)\rho']^2 + 2[n\rho + (n-1)\rho' \frac{d'}{d}}$$

$x = 0.328d = 149.1004mm$

The second moment of the area of the cracked section

$$I_1 = \left(\frac{bh^3}{12}\right) = \left(\frac{300 \times 149.1004^3}{12}\right) = 82865969.19mm^4$$

$I_2 \approx 0$

$I_3 \approx 0$

$A_1 = b \times h = 300x149.1004 = 44730.11244mm^2$

$A_2 = n \times A_s = 6.45 \times 1810 = 11668.64516mm^2$

$A_3 = (n-1) \times A'_s = (6.45-1) \times 402 = 2191.112258mm^2$

$$y_1 = x - \frac{x}{2} = \frac{167.7308}{2} = 74.55019mm$$

$y_2 = d - x = 455 - 149.1004 = 305.8996mm$

$y_3 = x - d' = 149.1004 - 41 = 108.1004m$

Therefore : -

$I_{cr} = I_1 + I_2 + I_3 + (A_1 \times y_1^2) + (A_2 \times y_2^2) + (A_3 \times y_3^2)$

$I_{cr} = 1448957116mm^4$

V. CRACKING MOMENT

Check if the section has cracked or not.

$$M_{cr} = \frac{f_r I_g}{y_t}$$

$f_r = 2.6MPa$

$$M_{cr} = \frac{2.6 \times 3620155858.4665}{259.65} = 36.25kNm$$

VI. EFFECTIVE SECOND MOMENT OF THE AREA

$$I_e = \left(\frac{M_{cr}}{M_a}\right)^3 I_g + \left[1 - \left(\frac{M_{cr}}{M_a}\right)^3\right] I_{cr}$$

$$I_e = \left(\frac{36.25}{142.41}\right)^3 3620155858.4665 + \left[1 - \left(\frac{36.25}{142.41}\right)^3\right] 1448957116 = 1484766937.16853mm^4$$

VII. SHORTTERM DEFELECTION

$$\delta = \frac{5wl^4}{384E_c I_e}$$

$$\delta = \frac{5 \times 23.25 \times 7000^4}{384 \times 31000 \times 1484766937.16853} = 15.792mm$$

Table 3-4 Deflection in accordance to ACI with EC-2 material property

X/l	Moment [kNm]	I_e [mm^4]	δ [mm]
0.000	0.000	3620155858	0.000
0.100	51.266	2216546498	-3.321
0.200	91.140	1585571535	-8.783
0.300	119.621	1509379604	-12.631
0.400	136.710	1489435462	-14.992
0.500	142.406	1484769766	-15.792
0.600	136.710	1489435462	-14.992
0.700	119.621	1509379604	-12.631
0.800	91.140	1585571535	-8.783
0.900	51.266	2216546498	-3.321
1.000	0.000	3620155858	0.000

3.5 Calculation of Short Term Deflection in Accordance to Bischoff's Method

The same procedure is taken as in the ACI-318 but the effective moment of inertia is calculated in accordance to Equation 2.6, rewritten below.

$$\frac{1}{I_e} = \left(\frac{M_{cr}}{M_a}\right)^m \frac{1}{I_g} + \left[1 - \left(\frac{M_{cr}}{M_a}\right)^m\right] \frac{1}{I_{cr}} \geq \frac{1}{I_g}$$

Therefore, taking the same data as in section 3.4, the deflection along the beam span is computed and presented as follows.

Table 3-5 Deflection in accordance to ACI with Bischoff's Method

X/l	Moment [kNm]	I_e [mm^4]	δ [mm]
0.000	0.000	3833074063	0.000
0.100	51.266	3713385750	-2.731
0.200	91.140	2198712204	-8.726
0.300	119.621	2037352441	-12.893
0.400	136.710	1989987529	-15.460
0.500	142.406	1978209200	-16.330
0.600	136.710	1989987529	-15.460
0.700	119.621	2037352441	-12.893
0.800	91.140	2198712204	-8.726
0.900	51.266	3713385750	-2.731
1.000	0.000	3833074063	0.000

3.6 Comparison

x	δ ACI [mm]	δ ACI with EC2 material property [mm]	δ ACI with Bischoff's Method [mm]	δ EC2 [mm]
0	0.000	0.000	0.000	0.000
0.7	-2.708	-3.321	-2.731	-4.536
1.4	-8.774	-8.783	-8.726	-8.670
2.1	-13.143	-12.631	-12.893	-11.966
2.8	-15.781	-14.992	-15.460	-14.076
3.5	-16.670	-15.792	-16.330	-14.801
4.2	-15.781	-14.992	-15.460	-14.076
4.9	-13.143	-12.631	-12.893	-11.966
5.6	-8.774	-8.783	-8.726	-8.670
6.3	-2.708	-3.321	-2.731	-4.536
7	0.000	0.000	0.000	0.000

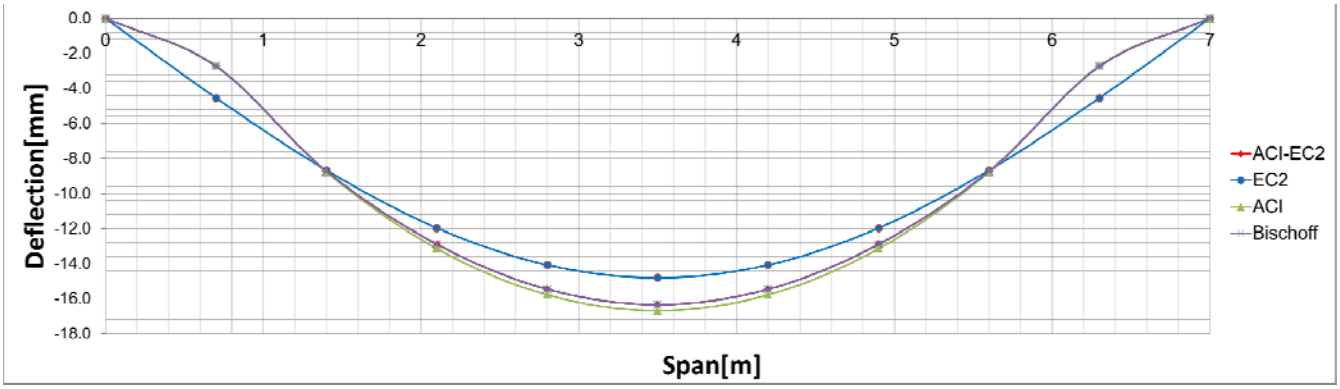

4. Introducing Tension Stiffening

4.1 Introduction

As discussed in section 2.1.5 the tensile capacity of concrete is typically neglected in strength design calculations, assuming that tensile forces are resisted entirely by the reinforcement at a crack. However, concrete continues to carry tension between the cracks through transfer of bond forces from the reinforcing bars into the concrete.

The concrete contribution between cracks is called tension stiffening, and this phenomenon has an effect on member stiffness, deflection, and crack widths under service load conditions.

From the experimental results of a research comparing a beam having a hallow core and solid cross section presents an interesting patterns of results. The comparison is made on the basis of load versus deflection.

The series of beams tested were of three kinds as shown in Figure 4-1,Figure 4-2 Pictures of the test specimens and Table 4-1:

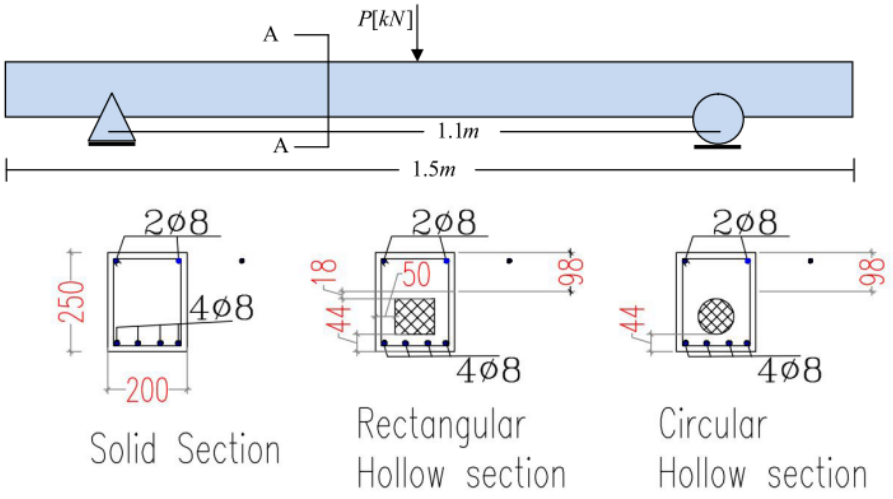

Figure 4-1 Geometry of the test specimens

Table 4-1Geometric parameters of the test specimens

Beam Section Type	Span Length [m]	Depth [m]	Width [m]
Solid	1.1	0.25	0.2
Circular Hollow	1.1	0.25	0.2
Rectangular Hollow	1.1	0.25	0.2

Figure 4-2 Pictures of the test specimens

The compressive strength of the concretes used in the three beams are tested and presented in Table 4-2.

Table 4-2 Cubic compressive strength of the concrete used in the three cross section types.

Beam Section Type	Cubic Concrete Strength [MPa]
Solid	29.84
Circular Hollow	44.7
Rectangular Hollow	44.7

As it can be deduced from the Table 4-2 the compressive results vary for the beam with the solid cross section versus the hollow cross sections. This was not intentional but had no implication on the mode of failure in the specimens. All three specimens failed by the rupture of the tensile reinforcements as shown in Figure 4-3.

a)

b)

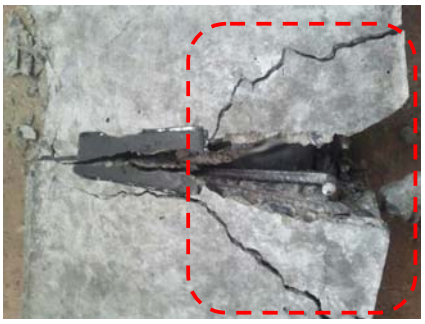

c)

Figure 4-3 Pictures of the test specimens after failure a) solid section, b) circular hollow section and c) rectangular hollow section

The load versus deflection data of the three beam tests is presented on:

Load [kN]	Deflection [mm]		
	SS	CHS	RHS
0	0	0	0
20	1.075	7.14	7.05
40	2.18	7.7	7.89
60	3.135	8.02	8.285
80	3.465	8.31	8.715
100	3.855	8.69	8.79
103	4.445	8.72	9.12
115	-	9.1	9.345

Tension stiffening is best understood by considering the axial response of a reinforced concrete tension member as illustrated in Figure 4-4. The member response is initially uncracked and governed more by the concrete than the reinforcement. Once cracked, the member response is affected by the reinforcing bar stiffness and follows a gradual transition toward the bare bar response as cracks develop in the member. Cracking is accompanied by a gradual reduction in average load carried by the concrete between cracks ($\overline{P}_c$) as more cracks develop. Once cracking has stabilized, the load carried by the concrete continues to decrease as secondary internal cracks develop between the primary cracks (Goto 1971; Bischoff 2001).

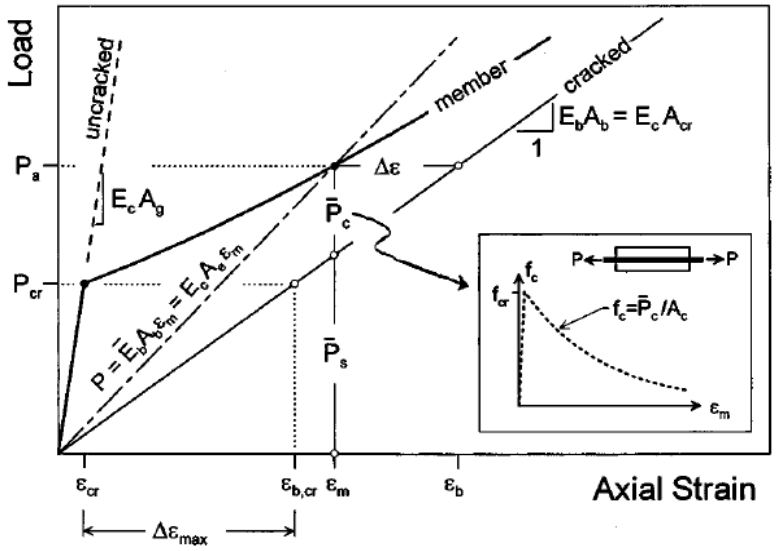

Figure 4-4 Tensile member response [5]

The effects of cracking and reinforcement on member stiffness can be taken into account a number of different ways. Most result in an effective member rigidity $(EA)_{eff}$.

I. The tension stiffening strain approach adopted by the CEB-FIP model code (CEB-FIP 1978, 1993) gives an effective modulus ($\overline{E}_b$) of embedded reinforcement with a bar area A_b. In this case

$$\overline{E}_b = \frac{E_b}{1-\beta_c\eta(P_{cr}/P_a)} = \frac{E_b}{1-\eta(P_{cr}/P_a)^2} \text{ with } \eta = 1-\frac{A_{cr}}{A_{unc}}, \beta_c = \frac{P_{cr}}{P_a} \qquad \textbf{Equation 4-1}$$

The axial member response is then predicted using $P = \overline{E}_b A_b \varepsilon_m$.

This method ignores the concrete tensile stresses but increases the apparent stiffness $\overline{E}_b$ of the reinforcement to account for the concrete contribution between cracks.

Expressing the effective member stiffness with a concrete modulus E_c and effective concrete area A_e gives:

$$A_e = \frac{A_{cr}}{1-\beta_c\eta(P_{cr}/P_a)} = \frac{A_{cr}}{1-\eta(P_{cr}/P_a)^2} \text{ with } \eta = 1 - \frac{A_{cr}}{A_{unc}},\ \beta_c = \frac{P_{cr}}{P_a} \qquad \textbf{Equation 4-2}$$

II. An alternative approach for modeling the postcracking member response is to account for the tensile contribution of concrete between cracks with an average stress-strain response for the cracked concrete (refer Figure 4-4). This gives a concrete tensile response with a descending branch after cracking and is equivalent to assuming the concrete has a reduced effective modulus of elasticity ($\overline{E}_c$) that depends on the level of strain in the member. Results from tests plotted in Figure 4-6 (Bischoff and Paixao 2004) show that the postcracking tensile strength of concrete $f_c = \beta_c f_{cr}$ is modeled reasonably well with

$$\beta_c = e^{-1100(\varepsilon_m - \varepsilon_{cr})(E_b/200)}$$

given the bar modulus E_b in GPa. This type of relationship based on member strains is not well suited for design and is more conducive to numerical solutions involving a detailed section analysis or use of finite elements.

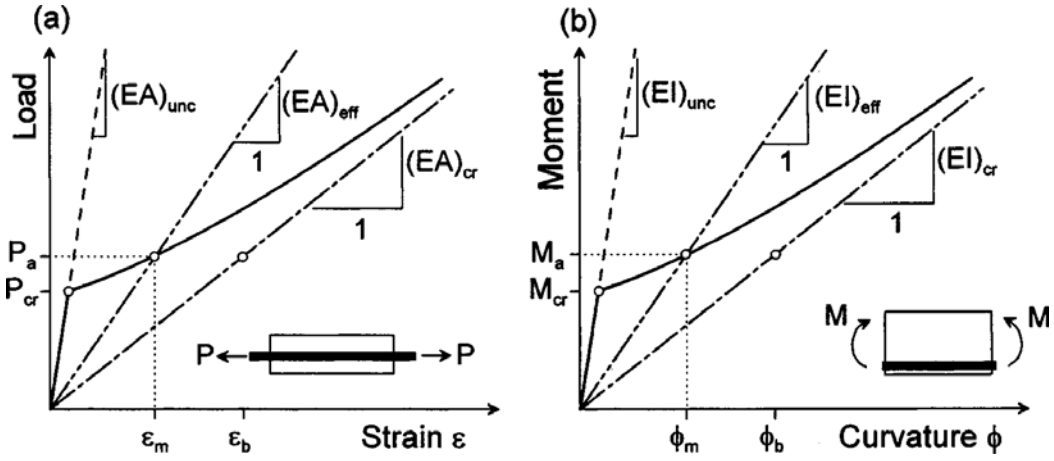

Figure 4-5 Member deformation for (a) axial member and (b) flexure member [5]

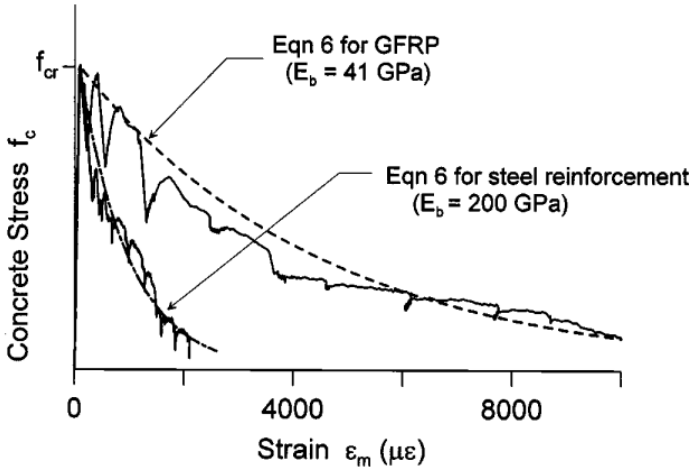

Figure 4-6 Postcracking response of concrete for steel and glass fiber reinforced polymer reinforced concrete (adapted from Bischoff and Paixao 2004) [5]

Instead of carrying out a detailed section analysis to determine the moment-curvature response for beams and modeling the concrete with an average postcracking tensile response to account for tension stiffening, it is more convenient to use an effective moment of inertia value s (I_e) using the same approach described for axial members in Figure 4-5. This gives:

$$I_e = \frac{I_{cr}}{1-\beta_c\eta(M_{cr}/M_a)} = \frac{I_{cr}}{1-\eta(I_{cr}/I_a)^2} \text{ with } \eta = 1 - \frac{I_{cr}}{I_{unc}},\ \beta_c = \frac{M_{cr}}{M_a}$$ **Equation 4-3**

Moment curvature is then predicted using $M = E_c I_c \Phi_m$.

Another approach to using an effective moment of inertia is to carry out a transformed section analysis using the effective modulus ($\overline{E}_b$) of the reinforcement to give an effective modular ratio $n = \overline{E}_b / E_c$. This is then used to calculate an effective value (I_{cr}) for the cracked transformed moment of inertia that is equivalent to I_e. For flexure

$$\overline{E}_b = \frac{E_b}{1-\beta_c\eta(M_{cr}/M_a)} = \frac{E_b}{1-\eta(M_{cr}/M_a)^2} \text{ with } \eta = 1 - \frac{I_{cr}}{I_{unc}}.\frac{d-c_{unc}}{d-c_{cr}},\ \beta_c = \frac{M_{cr}}{M_a}$$

Equation 4-4

III. Another approach is to model the developed the post cracking stress vs. strain relationship of concrete in tension using the smeared stress and strain relationship of concrete. [8] states a typical tensile stress–strain curve of concrete consists of two distinct branches. Before cracking the stress–strain relationship is essentially linear. After cracking, however, a drastic drop of strength occurs and the descending branch of the curve becomes concave. In

the descending branch, the concrete is cracked and the concept of concrete tensile stress σ_1^c and concrete tensile strain $\bar{\varepsilon}_1$ are quite different from those before cracking. σ_1^c is defined as the smeared (or average) concrete tensile stress and $\bar{\varepsilon}_1$ is the smeared (or average) concrete tensile strain.

Ascending branch ($\bar{\varepsilon}_1 \le \varepsilon_{cr}$)

$$\sigma_1^c = E_c \bar{\varepsilon}_1 \qquad \textbf{Equation 4-5}$$

Where:

$E_c =$ modulus of elasticity of concrete

$E_c = 3875\sqrt{f'_c(\text{MPa})}$

where f'_c and $\sqrt{f'_c}$ are in MPa.

ε_{cr} = cracking strain of concrete, taken as 0.00008 mm/mm

Descending branch ($\bar{\varepsilon}_1 > \varepsilon_{cr}$)

$$\sigma_1^c = f_{cr}\left(\frac{\varepsilon_{cr}}{\bar{\varepsilon}_1}\right)^{0.4} \qquad \textbf{Equation 4-6}$$

Where:

$f_{cr} =$ cracking stress of concrete, taken as $0.31\sqrt{f'_c(\text{MPa})}$

The above discussed methods can be summarized in to two categories.

1. Effective stiffness approach: in this approach the post cracking role of concrete is incorporated in a form of an effective moment of inertia or effective modulus of reinforcement after cracking.
2. Modeling the concrete with an average post cracking tensile response to account for tension stiffening.

In the following sections the above approaches are discussed and proposed to come up with the actual deflection values of the beam discussed in chapter 3 and the laboratory test beam specimen discussed in chapter 6.

4.2 Effective Stiffness Approach

Here under the tension stiffening effect is proposed to be incorporated in a form of an effective moment of inertia. This approach will be different from that of the Branson's (ACI-318) and Bischoff's approach as here the material property of the reinforcement is modified instead of the moment of inertia directly.

This is achieved by using the effective modulus ($\bar{E}_b$) of the reinforcement to give an effective modular ratio $n = \bar{E}_b / E_c$ which is then used to calculate an effective value (I_{cr}) for the cracked transformed moment of inertia that is equivalent to I_e.

The deflection calculation using this approach is illustrated as follows using the beam discussed in chapter 3.

4.2.1 Design data

Span = 7.0 m

G_k = 18.75 kN/m

Q_k = 15 kN/m

A'_s = 402 mm^2 ($2\phi 16$)

A_s = 1810 mm^2 ($4\phi 24$)

f_{ck} = 25 N/mm^2 (concrete strength class C25/30)

f_{yk} = 500N/mm^2 (Steel B500B)

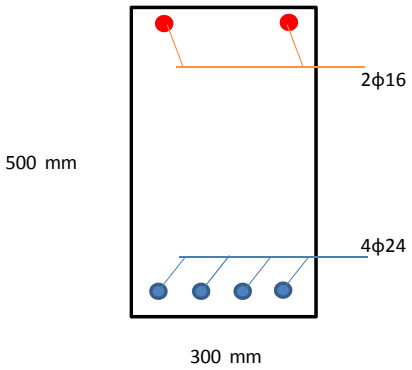

Figure 4-7 Cross-Section

4.2.2 Calculation Method

Here the deflection is calculated with elastic deflection equation using the modified stiffness of the member.

The stiffness is modified by means of the modular ratio which depends on the effective modulus of the steel corresponding to the service moment vs cracking moment.

4.2.3 Deflection Assessment

The procedure is, at frequent intervals along the member, to calculate

1) Moments

2) Deflections.

Here, calculations will be carried out at the mid-span position only, to illustrate this procedure, with values at other positions along the span being tabulated there after.

4.2.4 Calculation of Moments

$G_k + \psi_2 Q_k$

$\psi_2 = 0.3$

Therefore

Loading $= 18.75 + (0.3 \times 15) = 23.25 kN/m$

Mid-Span bending moment (M) $= \frac{23.25 \times 7^2}{8} = 142.41 kNm$

4.2.5 Calculation of Deflection

For concrete strength class C25/30, $E_{cm} = 31\text{kN/mm}^2$

$$n = \frac{\bar{E}_b}{31}$$

$$\bar{E}_b = \frac{E_b}{1-\beta_c\eta(M_{cr}/M_a)} = \frac{E_b}{1-\eta(I_{cr}/I_a)^2} \text{ with } \eta = 1-\frac{I_{cr}}{I_{unc}}.\frac{d-c_{unc}}{d-c_{cr}},\ \beta_c = \frac{M_{cr}}{M_a}$$

$\bar{E}_b = 200\text{GPa}$ when section is fully cracked

$$n = \frac{200}{31} = 6.45 \text{ when section is fully cracked}$$

$$\rho = \frac{A_s}{bd} = \frac{1810}{300\times 455} = 1.326\times 10^{-2}$$

$$\rho' = \frac{A'_s}{bd} = \frac{402}{300\times 459} = 2.919\times 10^{-3}$$

Having calculated the moment, the deflections may be calculated by using the elastic deflection equation as follows:

$$\delta = \frac{5wl^4}{384E_cI_e}$$

I. UNCKRACKED CROSS-SECTION

The neutral axis depth and the uncracked second moment of inertia are of the same value as calculated in section 3.2.3 and summarized below:

$x = 259.65mm$

$I_{unc} = 3620155858.4665mm^4$

II. FULLY CRACKED CROSS-SECTION

Neutral axis depth and second moment of the area of the fully cracked section are of the same value as calculated in section 3.2.3 and summarized below:

$x = 149.1004mm$

$I_c = 1448957116mm^4$

III. CRACKING MOMENT

Check if the section has cracked or not.

$$M_{cr} = \frac{f_{ctm}I_{unc}}{y_t}$$

$y_t = h - x = 500 - 259.65 = 240.35$

For concrete strength grade C25/30, $f_{ctm} = 2.6\text{N/mm}^2$

Therefore

$$M_{cr} = \frac{2.6\times 3620155858.4665}{240.35} = 39.2\text{kNm}$$

The section has cracked, since

$M_{cr} < M = 142.14kNm$

IV. EFFECTIVE SECOND MOMENT OF THE AREA

Cracked transformed cross section area.

$$\bar{E}_b = \frac{E_b}{1-\beta_c\eta(M_{cr}/M_a)} = \frac{E_b}{1-\eta(M_{cr}/M_a)^2} \text{ with } \eta = 1-\frac{I_{cr}}{I_{unc}}.\frac{d-c_{unc}}{d-c_{cr}},\ \beta_c = \frac{M_{cr}}{M_a}$$

$$\beta_c = \frac{M_{cr}}{M_a} = \frac{39.2}{142.14} = 0.27578$$

$$\left(\frac{M_{cr}}{M_a}\right)^2 = 0.07605$$

$$\eta = 1-\frac{I_{cr}}{I_{unc}}.\frac{d-c_{unc}}{d-c_{cr}} = 1-\frac{1448957116}{3620155858.4665}.\frac{455-259.65}{455-149.1004} = 0.74440$$

$$\bar{E}_b = \frac{E_b}{1-\eta(M_{cr}/M_a)^2} = \frac{200\text{GPa}}{1-(0.74440\times 0.07605)} = 212.00\text{GPa}$$

$$n = \frac{212}{31} = 6.84$$

The effective neutral axis depth:

$$\frac{1}{2}b(k_x d)^2 + (n-1)A'_s(k_x d - d') = nA_s(d-k_x d)$$

Dividing the above expression by bd^2 and denoting $\rho = A_s/bd$ and $\rho' = A_s/bd$ results in:

$$k_x = \frac{x}{d} = -[n\rho+(n-1)\rho'] + \sqrt{[n\rho+(n-1)\rho']^2 + 2[n\rho+(n-1)\rho'\frac{d'}{d}]}$$

$$x = 0.335d = 152.43mm$$

The second moment of the area of the cracked section

$$I_1 = \left(\frac{bh^3}{12}\right) = \left(\frac{300\times 152.43^3}{12}\right) = 88542413.85mm^4$$

$$I_2 \approx 0$$

$$I_3 \approx 0$$

$$A_1 = b\times x = 300x152.43 = 45729mm^2$$

$$A_2 = n\times A_s = 6.84\times 1810 = 12380.4mm^2$$

$$A_3 = (n-1)\times A'_s = (6.84-1)\times 402 = 2347.68mm^2$$

$$y_1 = x - \frac{x}{2} = \frac{152.43}{2} = 76.215mm$$

$$y_2 = d - x = 455 - 152.43 = 302.57mm$$

$$y_3 = x - d' = 152.43 - 41 = 111.43mm$$

Therefore :-

$$I_e = I_1 + I_2 + I_3 + (A_1\times y_1^2) + (A_2\times y_2^2) + (A_3\times y_3^2)$$

$$I_e = 1487125638mm^4$$

V. SHORTTERM DEFELECTION

$$\delta = \frac{5wl^4}{384E_c I_e}$$

$$\delta = \frac{5 \times 23.25 \times 7000^4}{384 \times 31000 \times 1487125638} = 15.767mm$$

Table 4-3 Deflection in accordance to the effective stiffness method

X/l	Moment [kNm]	β^2	E_b	n	np+(n-1)p'	2[np+(n-1)p'(d'/d)]	kx	x	I_e [mm^4]	δ [mm]
0.0	0.0	0.0	200000.0	6.5	0.1	0.2	0.3	149.1	1449783321.8	0.0
0.1	51.3	0.6	354123.9	11.4	0.2	0.3	0.4	183.1	2142399965.8	-3.4
0.2	91.1	0.2	231940.0	7.5	0.1	0.2	0.3	157.6	1589209951.8	-8.8
0.3	119.6	0.1	217377.0	7.0	0.1	0.2	0.3	153.9	1515203412.5	-12.6
0.4	136.7	0.1	213038.7	6.9	0.1	0.2	0.3	152.7	1492759610.1	-15.0
0.5	142.4	0.1	211955.4	6.8	0.1	0.2	0.3	152.4	1487125638.4	-15.8
0.6	136.7	0.1	213038.7	6.9	0.1	0.2	0.3	152.7	1492759610.1	-15.0
0.7	119.6	0.1	217377.0	7.0	0.1	0.2	0.3	153.9	1515203412.5	-12.6
0.8	91.1	0.2	231940.0	7.5	0.1	0.2	0.3	157.6	1589209951.8	-8.8
0.9	51.3	0.6	354123.9	11.4	0.2	0.3	0.4	183.1	2142399965.8	-3.4
1.0	0.0	0.0	200000.0	6.5	0.1	0.2	0.3	149.1	1424152137.0	0.0

4.3 Post-crack Tensile Property of Concrete

In this approach, as discussed early on this chapter, the post peak tensile property of concrete is modeled in accordance to the approach discussed in section 4.1.

4.3.1 Constitutive Law of Concrete under Tension

The complete stress vs strain diagram of concrete under tension is plotted using the procedure discussed in section 4.1.

Ascending branch ($\bar{\varepsilon}_1 \le \varepsilon_{cr}$)

$$\sigma_1^c = E_c \bar{\varepsilon}_1$$

Where:

E_c = modulus of elasticity of concrete

$E_c = 3875\sqrt{f'_c(\text{MPa})} = 3875\sqrt{25} = 19375\text{MPa}$

But here the value of the modulus of elasticity of concrete is taken as 31000N/mm^2

ε_{cr} = cracking strain of concrete, taken as 0.00008 mm/mm

$\sigma_1^c = 31000 \times \bar{\varepsilon}_1$

Concrete under Tension	
ε_1	σ_1
0	0
0.0000075	0.2325
0.000015	0.465
0.0000225	0.6975
0.00003	0.93
0.0000375	1.1625
0.000045	1.395
0.0000525	1.6275
0.00006	1.86
0.0000675	2.0925
0.000075	2.325
0.0000825	2.5575
8.3871E-05	2.6

Descending branch ($\bar{\varepsilon}_1 > \varepsilon_{cr}$)

$$\sigma_1^{\,c} = f_{cr}\left(\frac{\varepsilon_{cr}}{\bar{\varepsilon}_1}\right)^{0.4}$$

Where:

f_{cr} = cracking stress of concrete, taken as $0.31\sqrt{f'_c(\text{MPa})}$

$f_{cr} = 0.31\sqrt{25} = 1.55\text{MPa}$

But here the value for the fractur modulus is taken as 2.60 N/mm^2

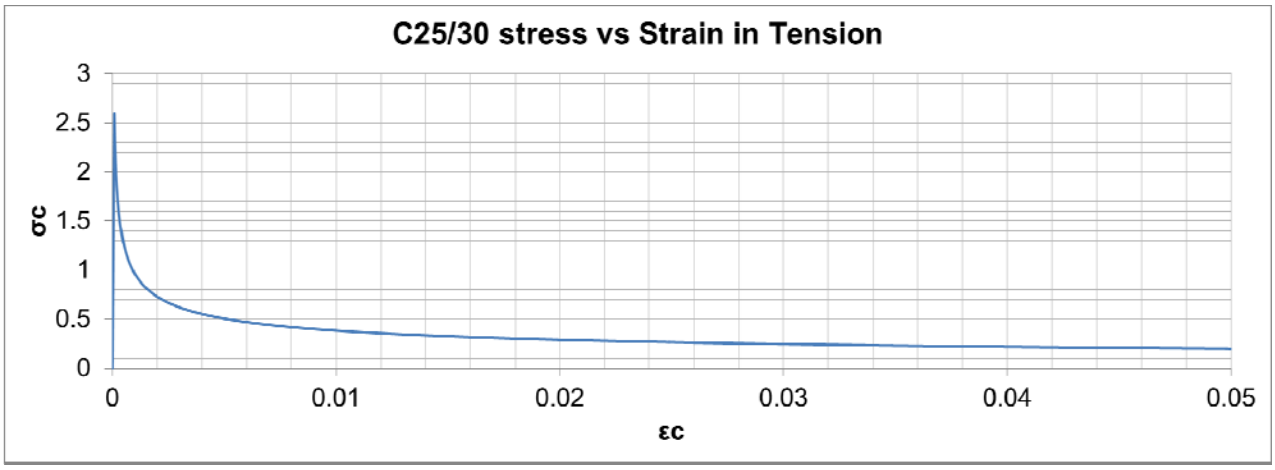

Figure 4-8 Stress vs. train diagram of concrete under tension

4.3.2 Constitutive Law of Bare Mild Steel under Tension

To plot the stress vs strain diagram of a bare reinforcing bar under tension Eurocode 2 is used. Based on section 3.2.7 of the code and using a steel grade of B500B we have the following diagram.

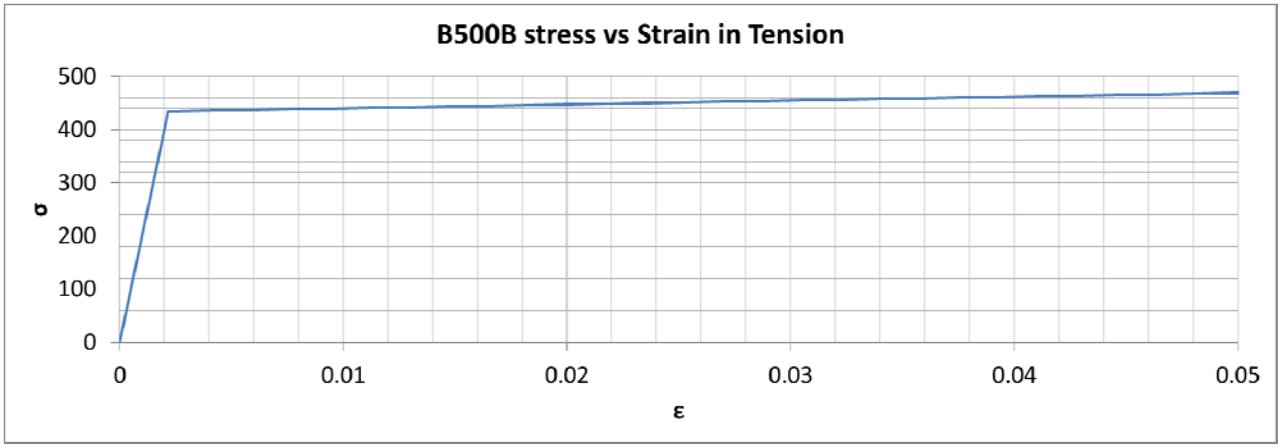

Figure 4-9 Stress vs. train diagram of bare reinforcing bar under tension

4.3.3 Smeared Stress-Strain Relationship of Mild Steel in Concrete

To come up with the smeared stress vs strain of a mild steel embedded in concrete the approach proposed by Thomas T. C. Hsu and Y. L. Mo [8] is as discussed as follows.

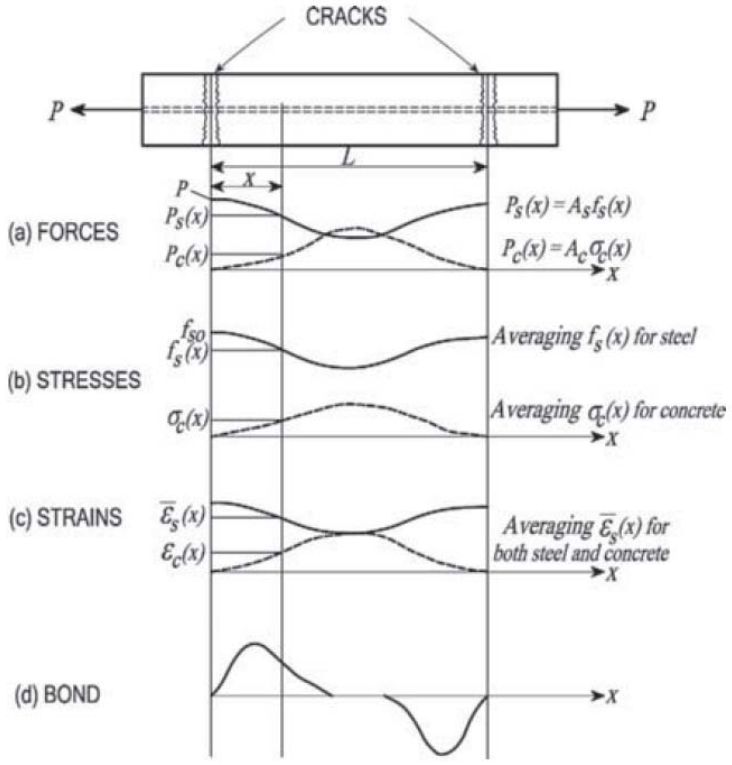

Figure 4-10 Stress and strains between two cracks [8]

Figure 4-10 shows the stress and strain distribution of a mild seel embeded in concrete and the surrounding concrete. After cracking, a portion of the tensile

member is isolated which includes two cracks with a spacing of L. At the two cracks indicated, the steel stress will be designated f_{so} , as indicated in Figure 4-10(b). At any section a distance x from the first left crack, however, the steel stress $f_s(x)$ will be less than f_{so}, and the difference will be carried by the concrete in tension $\sigma_c(x)$. The steel strain $\bar{\varepsilon}_s(x)$ and the concrete strain $\varepsilon_c(x)$ are also sketched in Figure 4-10 (c). The steel strain $\bar{\varepsilon}_s(x)$ decreases from a maximum at the crack to a minimum at the midpoint between the two cracks. In contrast, the concrete strain $\varepsilon_c(x)$ should be zero at the crack and increases to a maximum at the midpoint. The difference between $\bar{\varepsilon}_s(x)$ and $\varepsilon_c(x)$ is caused by the slip between the steel bar and the surrounding concrete. The slip results in the bond stresses sketched in Figure 4-10(d) and the gaps that constitute the cracks.

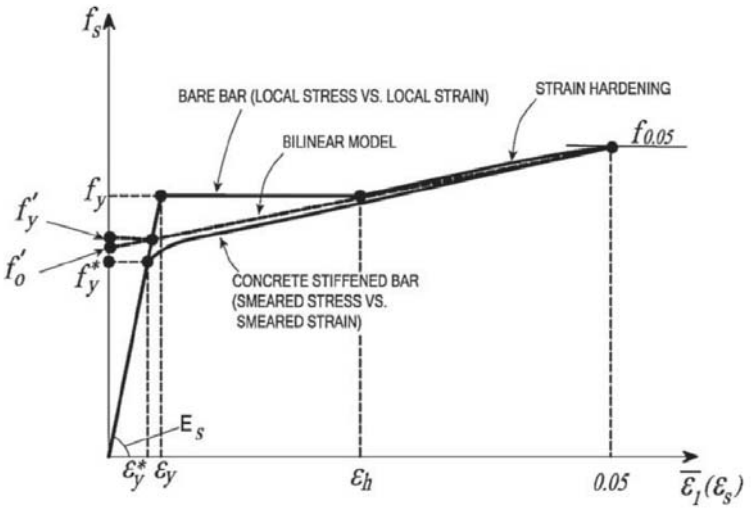

Figure 4-11 Stress and strains curve of mild steel [8]

The stress—strain relationship of mild steel bar tested in a bare condition exhibits a long plateau after yielding. However, the average stress-strain curve of steel bars embedded in concrete does not show such a yield plateau. The average stress at first yield called "apparent yield stress f_y*" and the average stresses in the post-yield range were found to be lower than those of a bare bar. This reduction of steel stress was found (Belarbi and Hsu, 1994) to be directly related to a parameter B = $(1/\rho)(f_{cr}/f_y)^{1.5}$ expressed in terms of steel and concrete tensile strengths (f_y and f_{cr}) as well as the reinforcement ratio (ρ).

$$\frac{f_y^*}{f_y} = 1 - \frac{4}{\rho}\left(\frac{f_{cr}}{f_y}\right)^{1.5} = 1 - 4B$$ **Equation 4-7**

4.3.3.1 Smeared Stress–Strain Curve of Mild Steel after Yield

The smeared stress–strain relationship of mild steel bars embedded in concrete is more difficult to determine after yielding, because the steel strain at the cracked sections increases rapidly to reach the strain hardening region of the stress–strain curve. The averaging of the steel strains and the corresponding steel stresses along the length L becomes mathematically more complex. The integration process involved in the averaging requires numerical integration and the use of an electronic computer.

In order to simplify the averaging process, two assumptions are made by Tamai et al. (1987).

a. The stress distribution in the steel between two adjacent cracks is assumed to follow a full cosine curve.
b. The smeared stress–strain relationship of concrete in tension (Equation 4-5 and 4-6), is valid both before and after yielding.

With the two assumptions we have the following distribution function for stress of the steel between two cracks.

$$f_s(x) = f_s + \frac{\sigma_c}{\rho}\cos\frac{2\pi x}{L}$$ **Equation 4-8**

With these two assumptions, the averaging process is summarized as follows:

1. Select a value of the smeared steel stress f_s.
2. Assume a smeared steel strain $\bar{\varepsilon}_s$.
3. Calculate the distribution of steel stress $f_s(x)$ from Equation (4-8).
4. Determine the corresponding distribution of steel strain $\bar{\varepsilon}_s(x)$ according to the stress–strain curve of bare bars (Section4.3.2).
5. Calculate the smeared steel strain $\bar{\varepsilon}_s$ by numerical integration of the following integral:

$$\bar{\varepsilon}_s = \frac{1}{L}\int_0^L \bar{\varepsilon}_s(x)dx$$ **Equation 4-9**

6. If $\bar{\varepsilon}_s$ calculated from Equation (4-9) is not the same as that assumed, repeat step 2–5 until the calculated $\bar{\varepsilon}_s$ is sufficiently close to the assumed value. The calculated $\bar{\varepsilon}_s$ and the selected value f s provide one point on the smeared stress–strain curve in the post-yield range.
7. By selecting a series of f_s values and find their corresponding $\bar{\varepsilon}_s$ values from steps 2–6, the whole smeared stress–strain curve in the post-yielding range can be plotted.

As one could deduce from the procedure above coming up with the post apparent yield smeared stress v strain curve of a mild steel embedded in concrete is not an easy task and would require computers for the integration and averaging. To overcome this, a FORTRAN program is prepared for the purpose of this thesis as presented in Appendix A.

Another alternative to overcome this complication is to use the experimentally supported constitutive law proposed in [9].

$$f_s = E_s\varepsilon_s;\ \varepsilon_s \le \varepsilon_n$$

$$f_s = f_y\left[(0.91-2B)+(0.02+0.25B)\frac{\varepsilon_s}{\varepsilon_y}\right];\varepsilon_s \le \varepsilon_n \qquad \textbf{Equation 4-10}$$

$$\varepsilon_n = \varepsilon_y(0.93-2B)$$

$$B = \frac{1}{\rho}\left(\frac{f_{cr}}{f_y}\right)^{1.5}$$

To illustrate this method here under the smeared stress vs strain of a B500B reinforcemnt embeded in the tension zone of the beam section discussed in capter 3 is ploted.

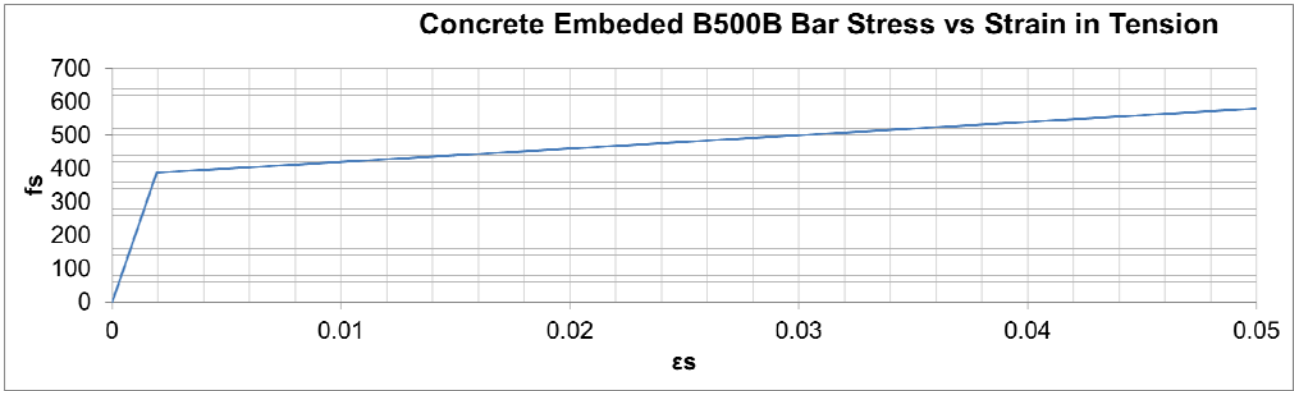

Figure 4-12 Stress vs. strain diagram of bare reinforcing bar under tension

Using the constitutive law of concrete in tension and reinforcement embedded in concrete we can plot the smeared stress vs strain diagram of the cross section in tension zone. This is

achieved by superimposing the stress of a concrete and an embedded reinforcement for the same strain value using the following derivation. The variables defined can be related with Figure 4-10.

$$P = P_s(x) + P_c(x)$$

$$A_s f_{so} = A_s f_s(x) + A_c \sigma_c(x)$$

where:

A_s = cross-sectional area of steel bars

A_c = area of net concrete sectional, not including A_s

Once A_c is determined the combined effect of the reinforcement and the surrounding concrete in tension is calculated as follows.

$$f_{so} = f_s(x) + \frac{1}{\rho}\sigma_c(x) \qquad \textbf{Equation 4-11}$$

A. <u>Total concrete area below the neutral axis</u>

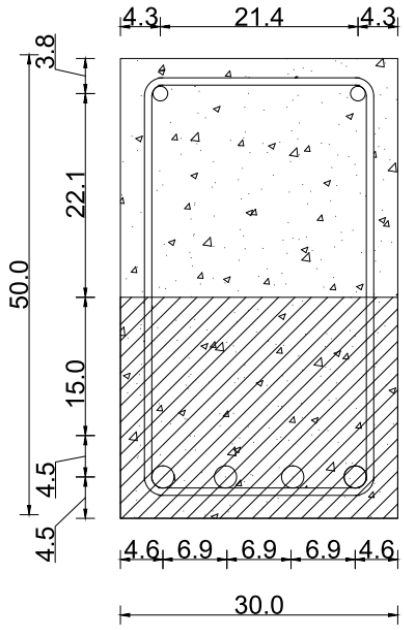

Figure 4-13 concrete section in the tension zone

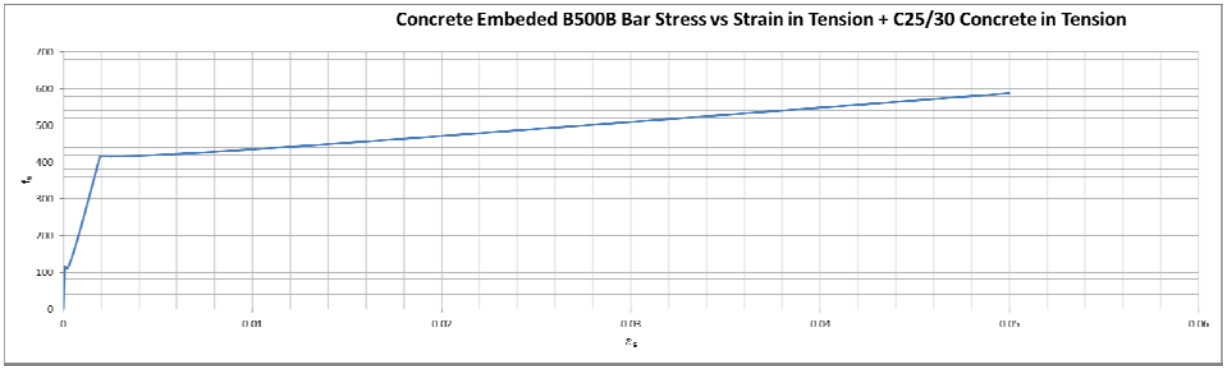

Figure 4-14 Stress vs. strain diagram reinforced concrete section in the tension zone

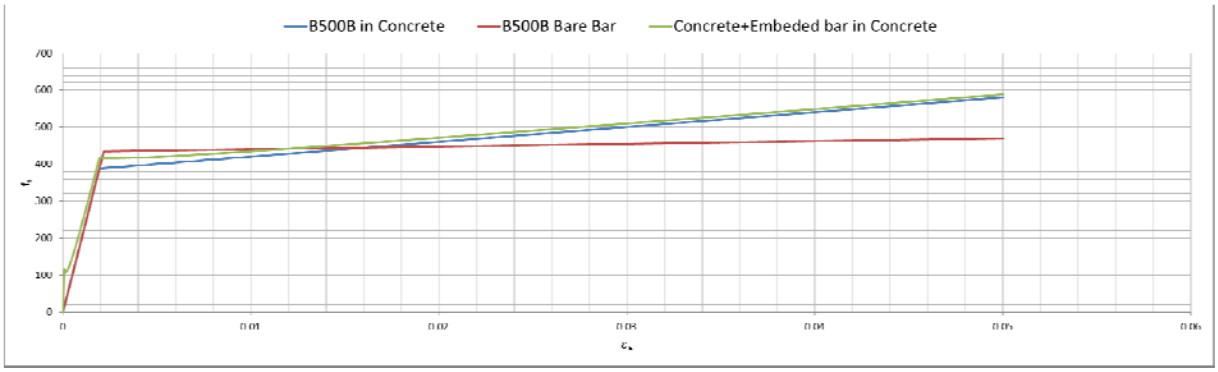

Figure 4-15 Comparison of the three stress vs. strain diagram in tension

In this approach, it should be noted that, the influence of the area of concrete has a major significance on the behavior of the surrounded reinforcement. This is not well incorporated in the methods discussed previously including the codes discussed in chapter 3.

But it is impractical to use the developed stress vs strain relationship of the new material in accordance to the methods discussed in sections 3.2, 3.3, 3.4, 3.5 and 4.2. To overcome this it is much convenient to convert the stress vs strain diagram to the tri-linear curve as shown below.

As one can observe the tri-linear curve developed has the following set of slopes along its path.

Table 4-4 Slope of tri-linear curve

Curve portion	Tri-linear slope [MPa]	Range [ε_{so}, σ_{so}]- [ε_{si}, σ_{si}] in (value, MPa)		Bare bar slope [MPa]
I	1000000	[0.0, 0.0]	[0.0000825, 82.5]	200000
II	176206	[0.00009, 81.44154]	[0.0019125, 402.577]	200000
III	3749.7	[0.00192, 405.4994]	[--,--]	29159.52

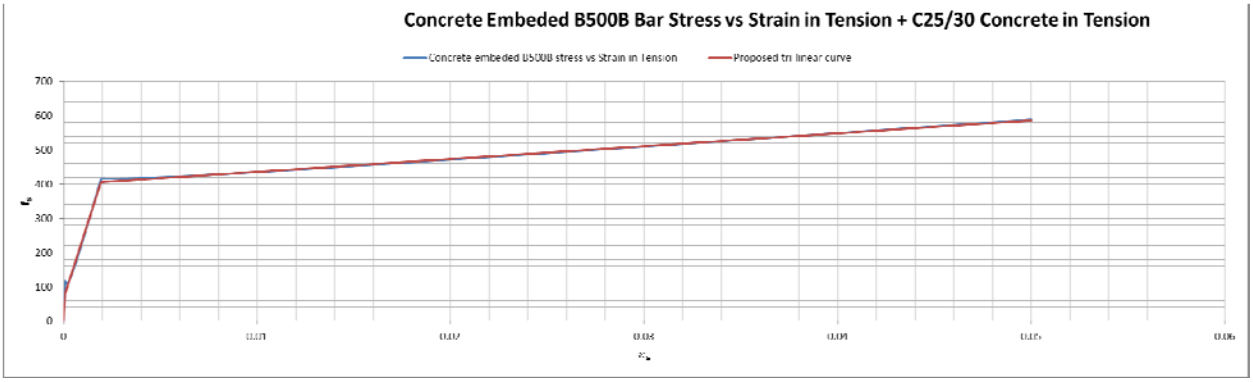

Figure 4-16 Proposed tri-linear curve considering the whole concrete area in the tension zone

The initial slope of proposed curve is significantly larger than the one used in codes this will definitely have an exaggerated difference in the deflection calculation. The author has realized that, it is unrealistic to consider the whole concrete section below the neutral axis having the same influence on the reinforcement embedded.

Therefore a more realistic portion of the concrete in the tension zone shall be considered. Here below two suggestions are discussed.

B. <u>Effective area bounded by distance from the center of the reinforcement to outer concrete fiber.</u>

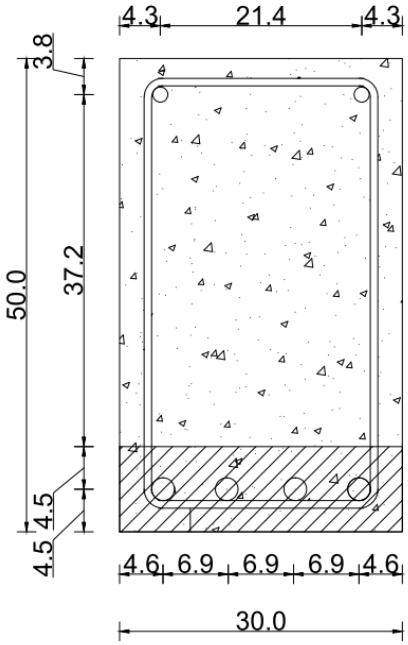

Figure 4-17 Proposed effective reinforced concrete section in the tension zone

The effective area proposed is the immediate surroundings, of the length equaling the distance from the center of the reinforcement to the other tension fiber of the concrete.

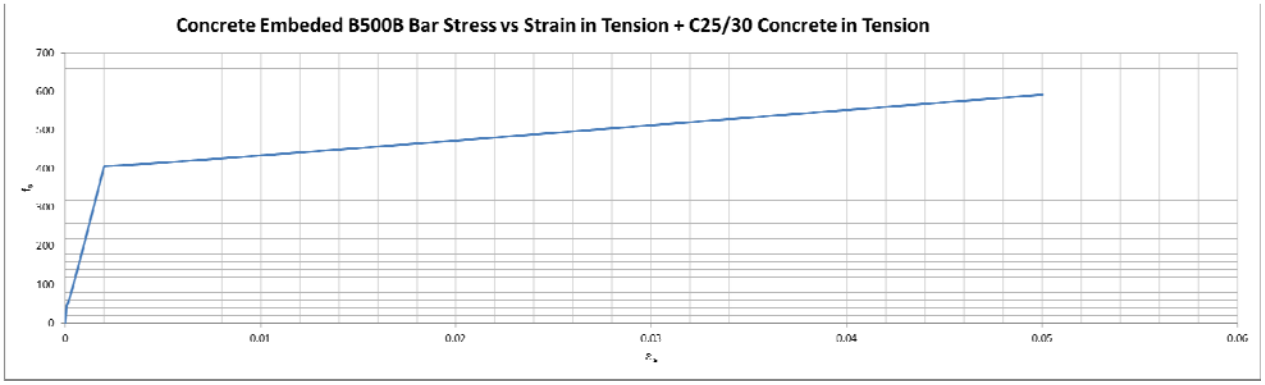

Figure 4-18 Stress vs. strain diagram proposed effective reinforced concrete section in the tension zone

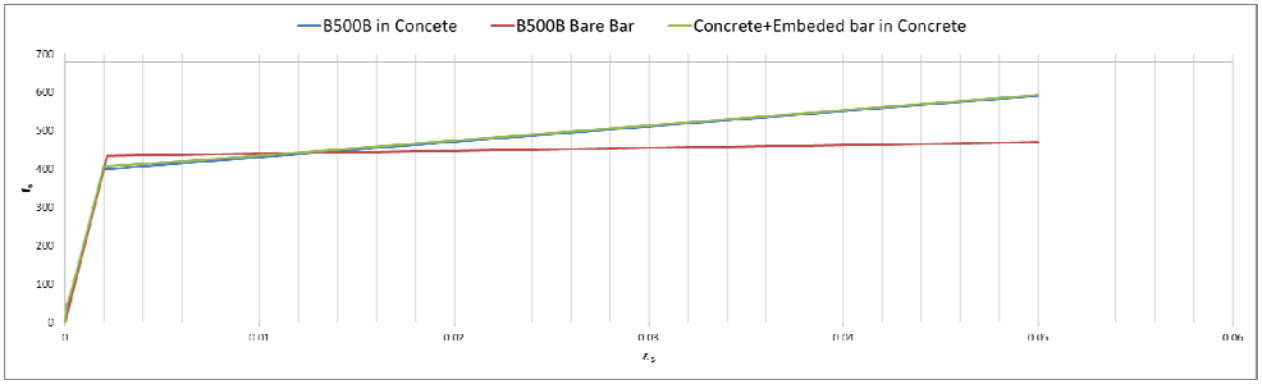

Figure 4-19 Comparison of the three stress vs. strain diagram in tension for the proposed effective concrete section in the tension zone

Table 4-5 Slope of tri-linear curve

Curve portion	Tri-linear slope [MPa]	Range [ε_{so}, σ_{so}]- [ε_{si}, σ_{si}] in (value, MPa)		Bare bar slope [MPa]
I	559326	[0.0, 0.0]	[0.0000825, 46.1444]	200000
II	192711	[0.00009, 37.43499]	[0.0019125, 388.6508]	200000
III	3924.8	[0.00192, 403.9751]	[--,--]	29159.52

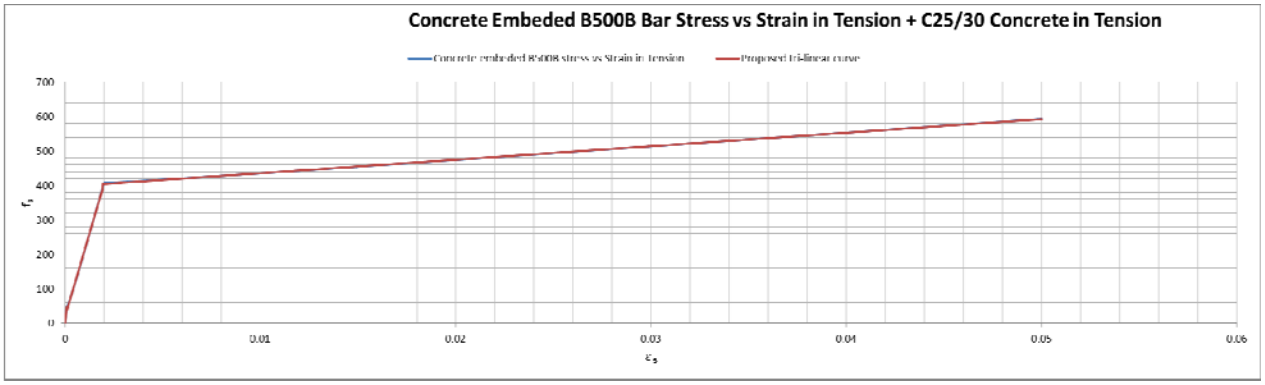

Figure 4-20 Proposed tri-linear curve considering the concrete area in proposed above

This is still unrealistic outcome as the elastic modules of elasticity is a little over twice the amount of the reinforcement.

As a result a final estimation of the effective area of concrete is considered.

C. Effective embedment zone of concrete.

This refers to the effective area of concrete surrounding the reinforcemnt that is infulenced by the bond. Different recommendations as to the extent of this zone are provided in different literatures. Here two extream cases are considered:

1. The effective embedment zone is the area of concrete around the reinforcing bar at the distance of 7.5 bar diameter. This is in accordance to the recommendation provided in CEP-FIP (1978) [16]. Accordingly the beam will have the following effective embedment zone.

   $c_d = 7.5 \times \text{Diameter of bar} = 7.5 \times 24 = 180mm$

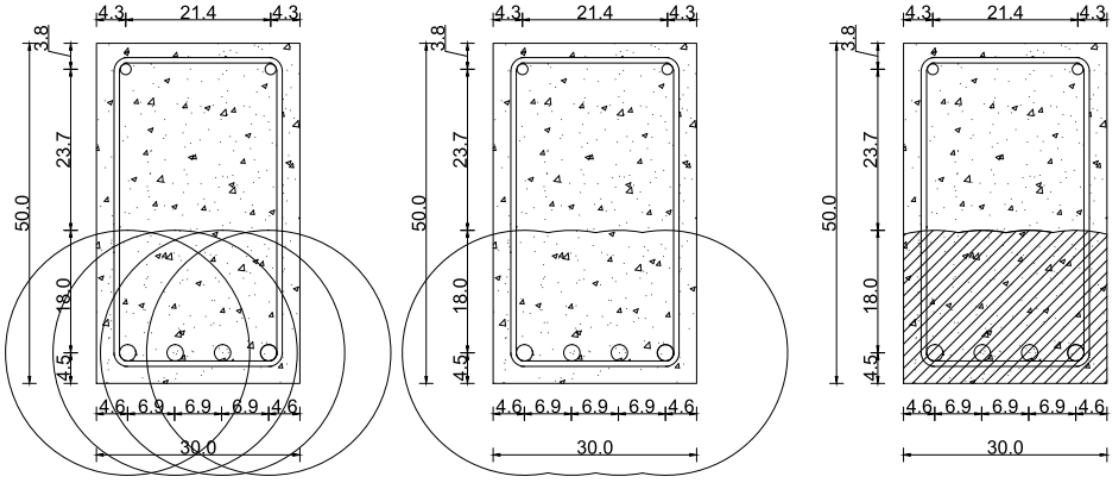

Figure 4-21 Proposed effective reinforced concrete section in the tension zone designated as proposed approach max.

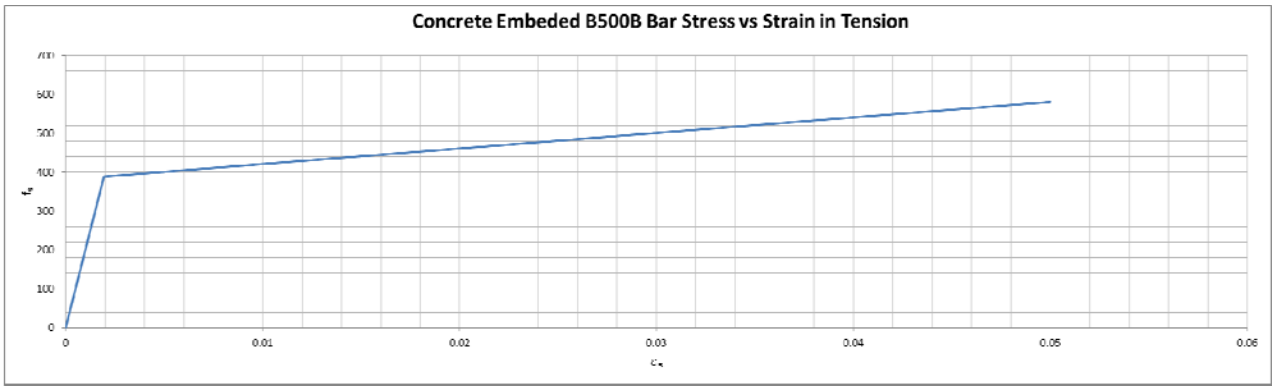

Figure 4-22 Stress vs. strain diagram proposed effective reinforced concrete section in the tension zone designated as proposed approach max.

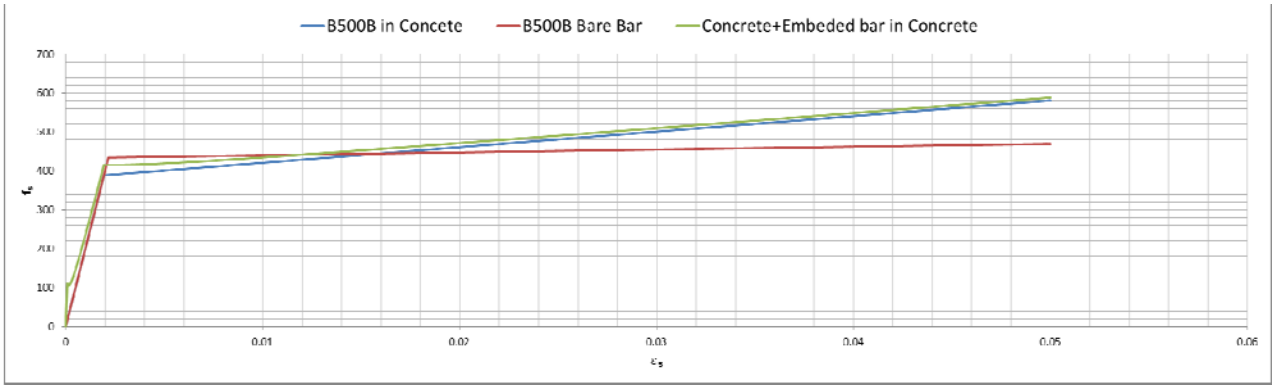

Figure 4-23 Comparison of the three stress vs. strain diagram in tension for the proposed effective concrete section in the tension zone designated as proposed approach max.

Table 4-6 Slope of tri-linear curve

Curve portion	Tri-linear slope [MPa]	Range [ε_{so}, σ_{so}]- [ε_{si}, σ_{si}] in (value, MPa)		Bare bar slope [MPa]
I	1000000	[0.0, 0.0]	[0.0000825, 82.5]	200000
II	177322	[0.00009, 78.459]	[0.0019125, 401.628]	200000
III	3791.5	[0.00192, 405.392]	[--,--]	29159.52

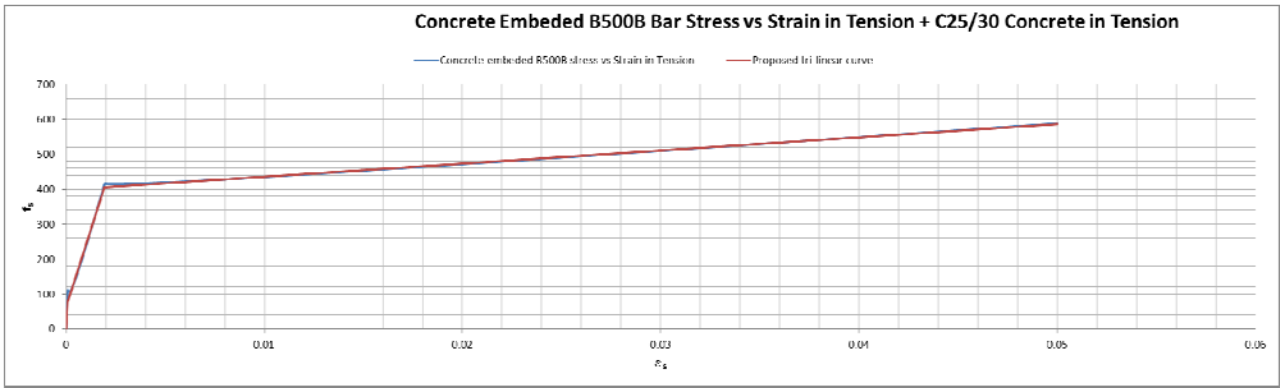

Figure 4-24 Proposed tri-linear curve considering the effective rc zone of the concrete below neutral axis designated as proposed approach max.

2. The effective area proposed in this case, is the immediate surroundings, corresponding to half the clear distance between the reinforcement bars. This is illustrated and calculated below.

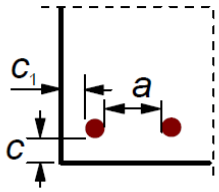

a) Straight bars

c_d = min (a/2, c_1, c)

$$c_d = \min(a/2, c_1, c)$$

$$c_1 = c = 25 + 8 = 33mm$$

$$a = \frac{300 - (25 + 25 + 8 + 8 + 24 + 24 + 24 + 24)}{2 \times 3} = 23mm$$

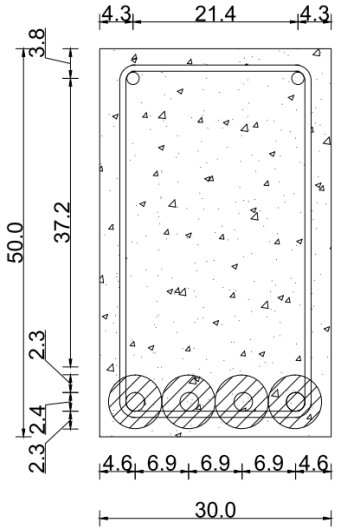

Figure 4-25 Proposed effective reinforced concrete section in the tension zone designated as proposed approach min.

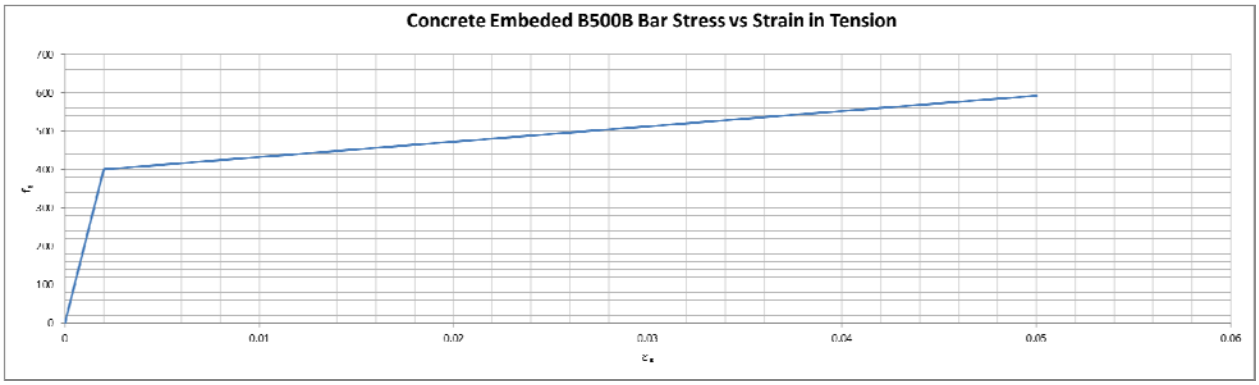

Figure 4-26 Stress vs. strain diagram proposed effective reinforced concrete section in the tension zone designated as proposed approach min.

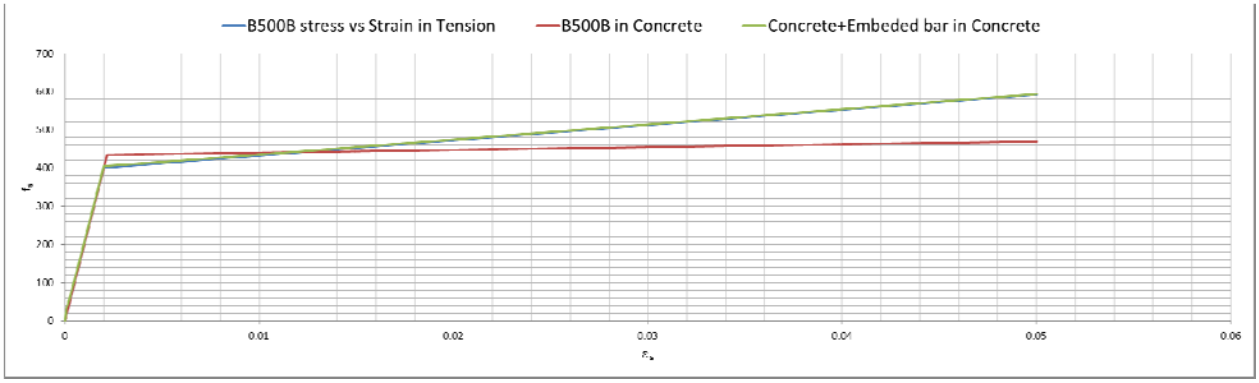

Figure 4-27 Comparison of the three stress vs. strain diagram in tension for the proposed effective concrete section in the tension zone designated as proposed approach min.

Table 4-7 Slope of tri-linear curve

Curve portion	Tri-linear slope [MPa]	Range [ε_{so}, σ_{so}]- [ε_{si}, σ_{si}] in (value, MPa)		Bare bar slope [MPa]
I	401540	[0.0, 0.0]	[0.0000825, 28.901]	200000
II	195912	[0.00009, 28.9011]	[0.0019125, 385.9507]	200000
III	3959	[0.00192, 403.6413]	[--,--]	29159.52

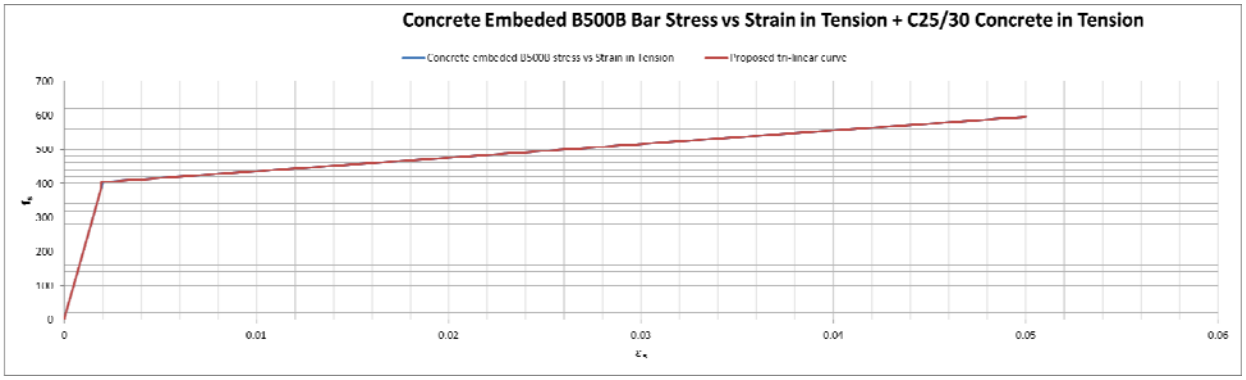

Figure 4-28 Proposed tri-linear curve considering the effective rc zone of the concrete below neutral axis designated as proposed approach min.

4.3.3.2 Influence of concrete surrounding the reinforcement

To illustrate the influence of the area of concrete surrounding the reinforcement, here under three tension members are proposed. All of them are 1200mm diameter 20 B500B reinforcements bar embedded in;

i. 100x100mm,
ii. 200x200mm and
iii. 300x300mm C25/30 concrete.

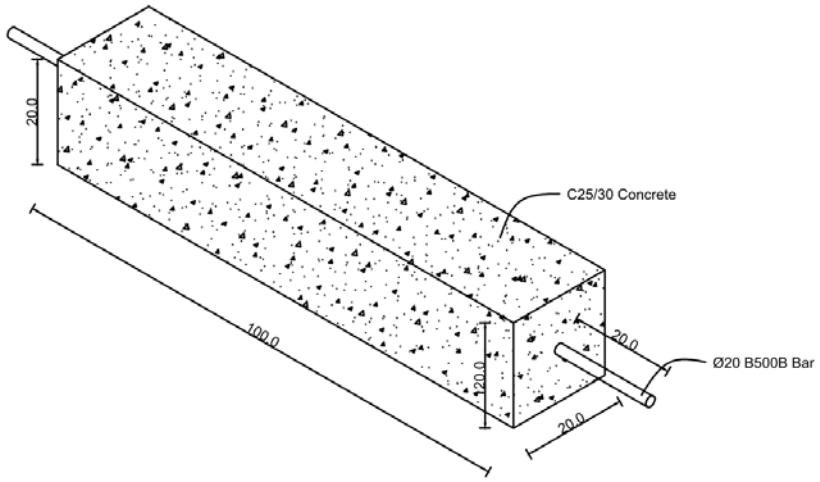

Figure 4-29 3D presentation of the tension member proposed

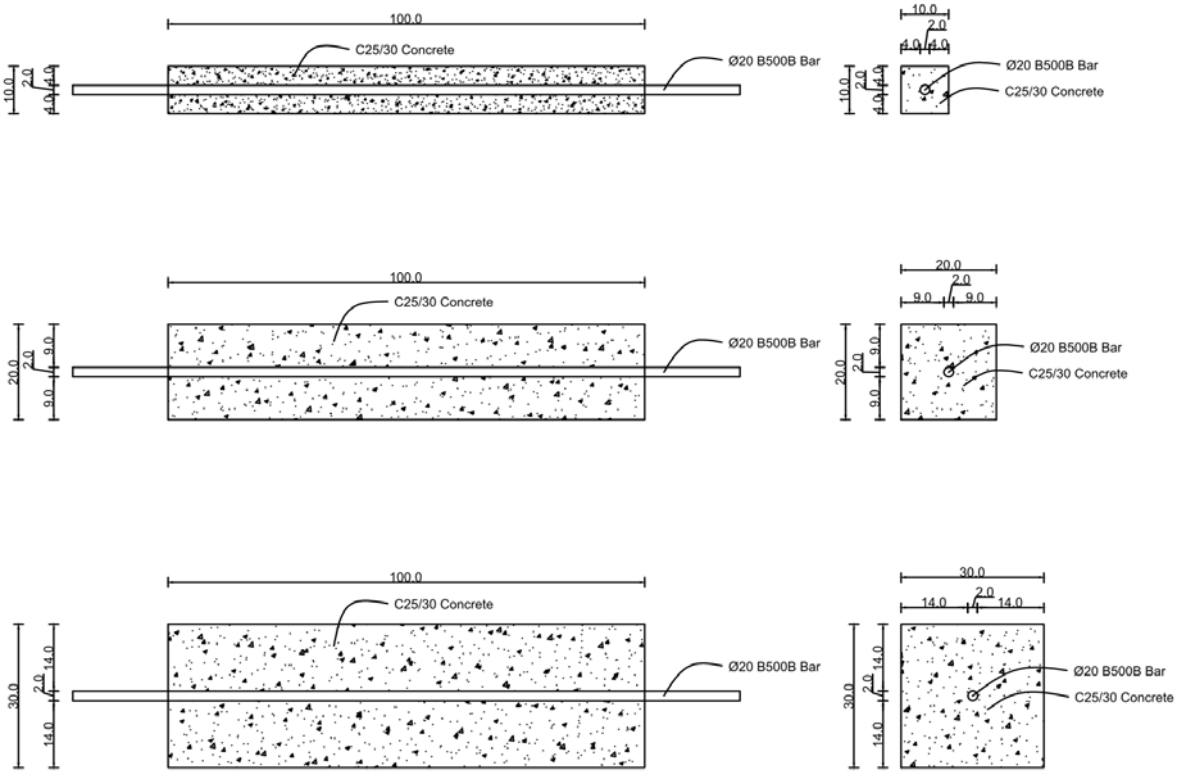

Figure 4-30 Diameter 20 B500B bar embedded in (a) 100x100mm, (b) 200x200mm and (a) 300x300mm C25/30 concrete

Following the same procedure discussed in section 4.3.3.1 the smeared stress vs strain diagram of diameter 20 bar embedded in C25/30 concrete of varying size.

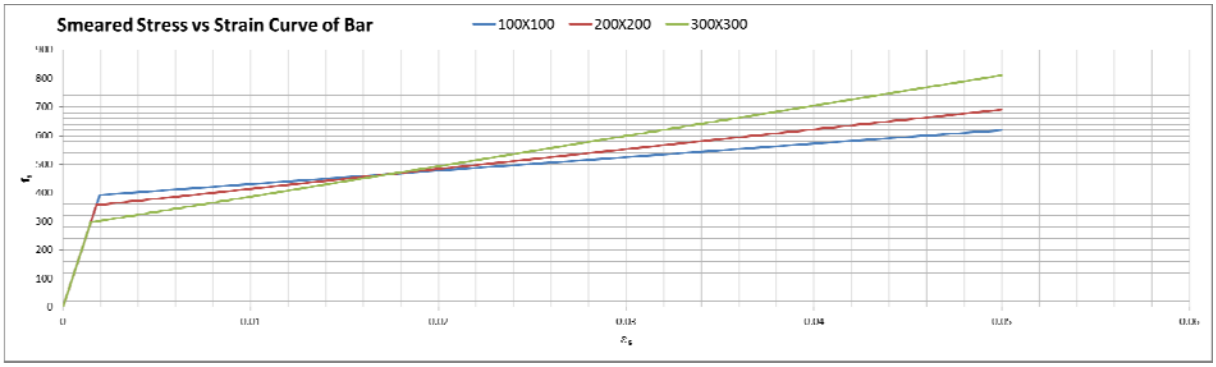

Figure 4-31 Diameter 20 B500B bar embedded in (a) 100x100mm, (b) 200x200mm and (a) 300x300mm C25/30 concrete

4.3.4 Proposed Calculation Method

Here the deflection is calculated with elastic deflection equation using the modified modulus of elasticity of the steel embedded in the concrete.

This is manifested in the modular ratio which depends on the effective modulus of the steel corresponding to the service stress vs cracking stress of concrete.

4.3.5 Deflection Assessment

As implied earlier the procedure is, at frequent intervals along the member, to calculate

1) Moments/stress
2) Deflections.

Here, calculations will be carried out at the mid-span position only, to illustrate this procedure, with values at other positions along the span being tabulated there after.

4.3.6 Calculation of Moments

$G_k + \psi_2 Q_k$

$\psi_2 = 0.3$

Therefore

Loading $= 18.75 + (0.3 \times 15) = 23.25 kN/m$

Mid-Span bending moment (M) $= \dfrac{23.25 \times 7^2}{8} = 142.41 kNm$

4.3.7 Calculation of Deflection

For concrete strength class C25/30, $E_{cm} = 31 kN/mm^2$

$$n = \frac{E_s}{31}$$

$E_s = 401.54GPa$ when $\sigma_s \leq 28.90MPa$

$$n = \frac{401.54}{31} = 12.9$$

$$\rho = \frac{A_s}{bd} = \frac{1810}{300 \times 455} = 1.326 \times 10^{-2}$$

$$\rho' = \frac{A'_s}{bd} = \frac{402}{300 \times 459} = 2.919 \times 10^{-3}$$

Having calculated the moment, the deflections may be calculated by using the elastic deflection equation as follows:

$$\delta = \frac{5wl^4}{384E_c I_e}$$

I. PROPOSED TRANSFORMED CROSSECTION ($\sigma_s \leq 28.90MPa$)

The neutral axis depth and the effective second moment of inertia:

$x = 190.9799mm$

$I_i = 2437657179mm^4$

II. PROPOSED TRANSFORMED CROSSECTION ($\sigma_s > 28.90MPa$)

Neutral axis depth and second moment of the area of the section are:

$x = 147.9425mm$

$I_{ii} = 1425937090mm^4$

III. CHECK IF $\sigma_s > 28.90MPa$

$$M = \frac{\sigma_s I_i}{y_t}$$

$$\sigma_s = \frac{My_t}{I_i}$$

$y_t = h - x = 500 - 190.9799 = 309.0201mm$

$$\sigma_s = \frac{142140000 \times 309.0201}{2437657179} = 18.02N/mm^2$$

$\sigma_s > 28.90N/mm^2$

IV. EFFECTIVE SECOND MOMENT OF THE AREA

Since $\sigma_s < 28.90N/mm^2$

$I_e = I_i = 2437657179mm^4$

V. SHORTTERM DEFELECTION

$$\delta = \frac{5wl^4}{384E_c I_e}$$

$$\delta = \frac{5 \times 23.25 \times 7000^4}{384 \times 31000 \times 2437657179} = 9.62mm$$

Table 4-8 Deflection in accordance to the proposed approach with minimum embedment zone.

X/l	Moment [kNm]	σ_s[N/mm^2]	E_s	I_e [mm^4]	δ [mm]
0.000	0.000	0.00000	401540	2437657179	0.000
0.100	51.266	6.49899	401540	2437657179	-3.020
0.200	91.140	11.55375	401540	2437657179	-5.713
0.300	119.621	15.16430	401540	2437657179	-7.821
0.400	136.710	17.33063	401540	2437657179	-9.160
0.500	142.406	18.05274	401540	2437657179	-9.619
0.600	136.710	17.33063	401540	2437657179	-9.160
0.700	119.621	15.16430	401540	2437657179	-7.821
0.800	91.140	11.55375	401540	2437657179	-5.713
0.900	51.266	6.49899	401540	2437657179	-3.020
1.000	0.000	0.00000	401540	2437657179	0.000

Similarly considering the maximum embedment zone area proposed by CEO-FIP code we can carry out the same procedure above and end up with results below.

Table 4-9 Deflection in accordance to the proposed approach with maximum embedment zone.

X/l	Moment [kNm]	σ_s[N/mm^2]	E_s	I_e [mm^4]	δ [mm]
0.000	0.000	0.00000	1000000	4563141429	0.000
0.100	51.266	2.81006	1000000	4563141429	-1.613
0.200	91.140	4.99566	1000000	4563141429	-3.052
0.300	119.621	6.55681	1000000	4563141429	-4.178
0.400	136.710	7.49350	1000000	4563141429	-4.893
0.500	142.406	7.80573	1000000	4563141429	-5.138
0.600	136.710	7.49350	1000000	4563141429	-4.893
0.700	119.621	6.55681	1000000	4563141429	-4.178
0.800	91.140	4.99566	1000000	4563141429	-3.052
0.900	51.266	2.81006	1000000	4563141429	-1.613
1.000	0.000	0.00000	1000000	4563141429	0.000

4.4 Comparison

From the results of section 4.3.4 we can have the following table summarizing the deflection calculation carried out for the 7m long beam.

Table 4-10 Summary of the deflection calculation carried out in the paper.

x	δ ACI [mm]	δ ACI with EC2 material property [mm]	δ ACI with Bischoff's Method [mm]	δ EC2 [mm]	δ proposed tension stiffening approch with min. embedment zone [mm]	δ proposed tension stiffening approch with max. embedment zone [mm]	Diffrence with min. embedment zone [%]	Diffrence with max. embedment zone [%]
0	0.000	0.000	0.000	0.000	0.000	0.000	0.00	0.00
0.7	-2.708	-3.321	-2.731	-4.536	-3.020	-1.613	33.44	64.44
1.4	-8.774	-8.783	-8.726	-8.670	-5.713	-3.052	34.11	64.80
2.1	-13.143	-12.631	-12.893	-11.966	-7.821	-4.178	34.64	65.08
2.8	-15.781	-14.992	-15.460	-14.076	-9.160	-4.893	34.92	65.24
3.5	-16.670	-15.792	-16.330	-14.801	-9.619	-5.138	35.01	65.28
4.2	-15.781	-14.992	-15.460	-14.076	-9.160	-4.893	34.92	65.24
4.9	-13.143	-12.631	-12.893	-11.966	-7.821	-4.178	34.64	65.08
5.6	-8.774	-8.783	-8.726	-8.670	-5.713	-3.052	34.11	64.80
6.3	-2.708	-3.321	-2.731	-4.536	-3.020	-1.613	33.44	64.44
7	0.000	0.000	0.000	0.000	0.000	0.000	0.00	0.00

As the results imply the deflection is significantly small when calculated considering the role of concrete still intact between consecutive cracks.

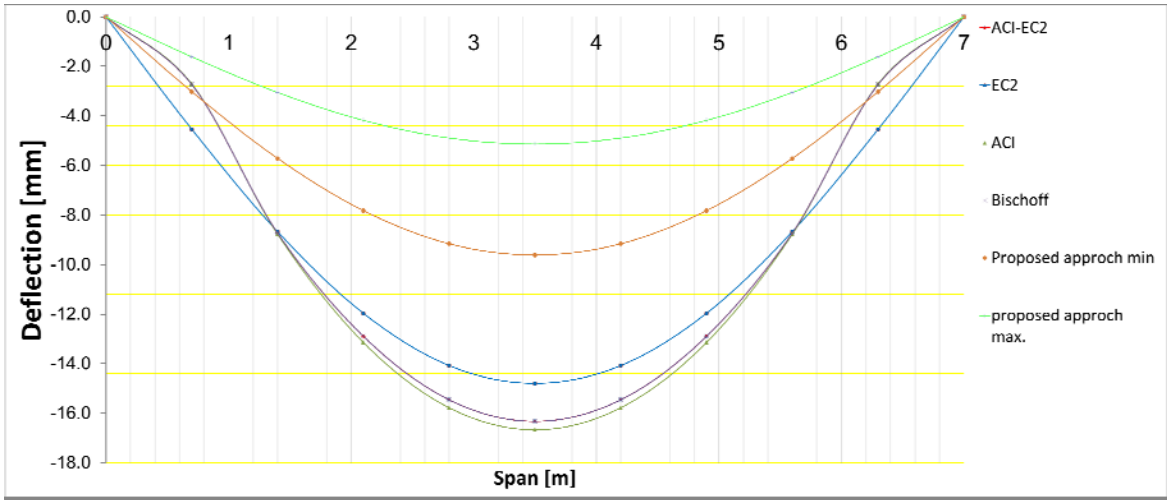

5. Conclusion and Recommendation

5.1 Observation and Conclusion

With the present trend of use of higher strength concrete and reinforcement, leading to longer spans and smaller depths, deformations are often the governing design criterion. Accurate deformation estimations are needed not only for deflection calculation, but also for more accurate numerical simulation of load carrying capacity of some structures. An adequate modelling of concrete cracking and, particularly, post-cracking behaviour, as one of the major sources of nonlinearity, is the most important task of deformational analysis. In this regards, the following observations and conclusions are made.

1) Design codes (EN 2004 and ACI 318 2008) are based on different assumptions and methods for strength, cracking and deformation analysis. Although these methods ensure safe design, they do not reveal the actual stress-strain state of cracked structures and often lack solid interpretation. This leads to an over estimation of deflection.
2) The discussed design codes and methods address deflection as the function of the section that will behave in a state between fully intact or fully cracked, depending on its state of stress. But these approaches fail to fully incorporate the tension stiffening effect which mainly is the attribute of the intact concrete between cracked sections.
3) Numerical methods which were rapidly progressing are based on universal principles and can include all possible effects such as material nonlinearities, concrete cracking, creep and shrinkage, reinforcement slip, etc. However, the progress is mostly related to the development of mathematical tool, but not material models. A very good example of this would be the difference on how a bare bar and the same bare in concrete behave under tension.
4) The proposed approach of using the smeared stress vs strain model of reinforcement in concrete to account for tension-stiffening law depends on concrete tensile strength and reinforcement ratio. Tension-stiffening reduces with increase in reinforcement ratio, but increases with tensile strength of concrete.

5.2 Recommendation

The proposed approach is based on the smeared stress vs strain relationship of reinforcement in concrete and that of the concrete in the effective embedment zone. These constitutive laws were the result of intensive works by Hsu T.C. Thomas [8]. This paper investigated an approach to adopt these laws in calculating the immediate deflection of a reinforced concrete beam under service load. And from the results the flowing recommendations are put forward by the author:

1. Deflection of reinforced concrete flexural members is more of a member property rather than a section. And this is mainly due to the composite nature of reinforced concrete. Whereas the section approach is more suited for flexural members made out of elastic homogenous materials.
2. In addition to the above point, the influence concrete on the embedded reinforcement is highly dependent on the bond between them. Current studies are trying to address on how this bond can be realistically modeled. But it has not yielded in to a universally accepted law. Hence further development in this regards can help shade light on how effectively can concrete be used intension zone.
3. The effective area of concrete in tension provided in codes and standards do not specify whether it is equally effective in the tension stiffening phenomenon or not. Hence, a clear demarcation of the effective concrete area in tension and the effective embedment zone should be addressed for a better understanding of tension stiffening for everyday design practice by the professional.
4. This paper only focused on the role of concrete in tension and fully acknowledges that other parameters such as variation in load, confinement effect of shear reinforcement, shrinkage and other time dependent factors like creep and maturing process of concrete have a significant role in the long run. Therefore the author plans to address such issues in future works.

Appendix A

FORTRAN PROGRAM for Smeared Strain Calculation

```
!ADDIS ABABA UNIVERSITY
!Addis Ababa institute of Technology
!School of Civil and Environmental Engineering
!Yisshak Tadesse-GSR/1815/05
program Smeared_Stress_Strain_Curve_of_Mild_Steel_Embeded_in_Concrete
implicit none
! Variables are declared.
real::
fyk,Es=200000,fyd,C,fck,Ec,fcr,ecr=0.00008,As,Ac,ro,C1,fsx(1000),esx(1000),fs,es
,fyy
real,Parameter:: pi=3.1415927
integer::i,j,k
! Data entry
Print*, "please enter the following material properties and cross sectional
parameters"
Print*, "the class of concrete in use(limited from C15 to C60). e.g for C25 input 25"
Read*,C
fck=C/1.25
fcr=0.31*sqrt(fck)
Ec=9500*((fck+8)**(1.0/3.0))
Print*, "summary of the concrete property used"
Print*, "fck=",fck,"Mpa"
Print*, "fcr=",fcr,"Mpa"
Print*, " Ec=",Ec,"Mpa"
Print*, "ecr=",ecr,"mm/mm"
Print*, "_____________________________________________________________"
Print*, "the grade of reinforcing bar used. e.g. for S300 input 300"
Read*,fyk
fyd=fyk/1.15
Print*, "summary of the reinforcing bar property used"
Print*, "fyk=",fyk,"Mpa"
Print*, "fyd=",fyd,"Mpa"
Print*, " Es=",Es,"Mpa"
Print*, "_____________________________________________________________"
Print*, "area of reinforcement in tension zone in mm2"
Read*,As
Print*, "area of concrete in tension zone in mm2"
Read*,Ac
ro= As/Ac
Print*, "reinforcement ratio is",ro
Print*, "_____________________________________________________________"
fyy=fyd*(1-((4/ro)*((fcr/fyd)**1.5)))
Print*, "Please enter the stress in MPa for which you would want to compute
corresponding smeared stress"
Read*,fs
IF(fs<fyy)then
es=fs/Es
```

```
Else
es= ((((0.02-(fyy/Es))/(fyk-fyy))*(fs-fyy))+(fyy/Es))
End if
Do i=1,10,1
C1=(1.0/ro)*fcr*((ecr/es)**0.4)
Do j=1,1000,1
fsx(j)=fs+(C1*cos(pi*(j/1000)))
End Do
Do k=1,1000,1
If(fsx(k)<fyd)then
esx(k)= fsx(k)/Es
else
esx(k)=fyd/Es
end if
End Do
es=sum(esx)/1000
End do
Print*,es
end program Smeared_Stress_Strain_Curve_of_Mild_Steel_Embeded_in_Concrete
```

References

[1] American Concrete Institute (ACI). (2008). "Building code Requirements for Structural Concrete." ACI 318-08, ACI Committee 318, Detroit.

[2] European Committee for Standardization (CEN). (1992). "Eurocode 2: Design of Concrete Structures-Part1-1; General Rules and Rules for Buildings." DD ENV 1992-1-1, European Prestandard, Brussels, Belgium.

[3] Gilbert, R. I. (2007). "Tension Stiffening in Lightly Reinforced Concrete Slabs" Journal of Structural Engineering,

[4] Gilbert, R. I. (2008). "Calculation of Long-Term Deflection" CIA Seminar.

[5] Bischoff, P.H. (2005). "Reevaluation of Deflection Prediction for Concrete Beams Reinforced with Steel and Fiber Reinforced Polymer Bars" Journal of Structural Engineering.

[6] Branson, D. E. (1965). "Instantaneous and time-dependent deflections of simple and continuous reinforced concrete beams." HPR Report No. 7, Part 1, Alabama Highway Department, Bureau of Public Roads, Alab. ~Dept. of Civil Engineering and Auburn Research Foundation, Auburn Univ., Aug. 1963.

[7] Kalkan Ilker. (2013). "Deflection prediction for reinforced concrete beams through different effective moment of inertia expressions" International Journal of Engineering Research and Development, Vol. 5, No. 1, January 2013

[8] Hsu T.C. Thomas and Mo Y.L. (2010)."Unified Theory of Concrete Structures" University of Houston, USA

[9] Belarbi Abdeldjelil, Zang Li-Xin and Hsu T.C. Thomas (1996). "Constitutive Laws of Reinforced Concrete Membrane Elements" Eleventh World Conference on Earthquake Engineering.

[10] Jendele L. Cervenka J. Saouma V. and Pulk R. "On the choice between discrete or smeared approach in practical structural FE analyses of concrete structures" University of Colorado at Boulder, USA.

[11] Sokolov Aleksandr (2010). "Tension Stiffening Model for Reinforced Concrete Beams" Vinus Technical University , Lithuania

[12] Khalfallah Salah and Guerdouh Dahbia (2014). "Tension Stiffening Approach in Concrete of Tensioned Members" International Journal of Advanced Structural Engineering.

[13] Behfarnia K. (2009). "The Effect of Tension Stiffening on the Behavior of R/C Beams." Asian Journal of Civil Engineering (Building and Housing) Vol. 10, NO. 3 Page 243-255

[14] Ng, PL, Lam, JYK and Kwan, AKH (2010). " Tension stiffening in concrete beams. Part 1: FE analysis" Institution of Civil Engineers.

[15] Ng, PL, Lam, JYK and Kwan, AKH (2010). " Tension stiffening in concrete beams. Part 2: Member analysis" Institution of Civil Engineers.

[16] CEP-FIP (1978). "Model Code for C0ncrete Structures: CEP-FIP International Recommendations Model Code 1990." Parus: Comite Euro-International du Beton. P348

DECLARATION

I hereby declare that the work presented in this thesis is my original work and has not been presented for a degree in any other University and that all sources of material used for the thesis have been duly acknowledged.

_____ _____

Yisshak Tadesse Date

(Candidate)

This is to certify that the above declaration made by the candidate is correct to the best of my knowledge.

_____ _____

Dr. Esayas G/Youhannes Date

(Thesis Advisor)